Centro de Investigación Científica y de Educación Superior de Ensenada, Baja California

Doctorado en Ciencias
Ciencias de la Vida
con orientación en Microbiología

Regulation of endocytosis in *Neurospora crassa* and its role in morphogenesis

Tesis
Para cubrir parcialmente los requisitos necesarios para obtener el grado de Doctor en Ciencias

Presenta

Marisela Garduño Rosales

Ensenada, Baja California, México
2022

Tesis defendida por

Marisela Garduño Rosales

y aprobada por el siguiente Comité

Dra. Rosa Reyna Mouriño Pérez
Directora de tesis

Dr. Salomón Bartnicki García

Dra. Olga Alicia Callejas Negrete

Dr. Brian Douglas Shaw

Dra. Astrid Nalleli Espino Vázquez

Dra. Ana Denise Re Araujo
Coordinadora del Posgrado en Ciencias de la Vida

Dr. Pedro Negrete Regagnon
Director de Estudios de Posgrado

Resumen de la tesis que presenta **Marisela Garduño Rosales** como requisito parcial para la obtención del grado de Doctor en Ciencias en Ciencias de la Vida con orientación en Microbiología.

Regulación de la endocitosis en *Neurospora crassa* y su papel en la morfogénesis

Resumen aprobado por:

_____

Dra. Rosa Reyna Mouriño Pérez

Directora de tesis

El presente estudio examina aspectos fundamentales de la endocitosis como un proceso involucrado en la morfogénesis y crecimiento polarizado. Se desarrolló un procedimiento de fotoblanqueamiento basado en FRAP (por sus siglas en inglés, Recuperación de Fluorescencia Post-Fotoblanqueamiento) para medir la endocitosis en hifas de *Neurospora crassa* que expresan la proteína endocítica fimbrina, etiquetada con la proteína verde fluorescente (FIM-1-GFP). Se calculó que, bajo condiciones de crecimiento estándar, cerca del 12.5% de la membrana plasmática descargada en el ápice se endocita en el subápice, con una ocurrencia promedio de 21.4 eventos endocíticos/min/μm^2 en un área del collar endocítico de 236.7 μm^2. El procedimiento FRAP se realizó también en hifas crecidas en escasez de nutrientes y se encontró una ocurrencia promedio de 30.4 eventos endocíticos/min/μm^2 en un área del collar endocítico de 79.1 μm^2. Adicionalmente, se midió la internalización del reportero de endocitosis FM4-64 y se encontró los mismos valores de intensidad de fluorescencia en ambas condiciones de nutrientes. Se siguió la germinación de conidios para descifrar el establecimiento del collar endocítico utilizando las cepas FIM-1-GFP y FIM-1-mChFP/CHS-1-GFP (quitina sintasa 1). Se encontró que al principio los parches endocíticos forman una capucha en la punta del germínula y cuando el tubo germinal alcanza una longitud de ~150 µm, el arreglo de los parches comienza a cambiar a un collar subapical. Adicionalmente, se realizaron experimentos de daño mecánico en hifas maduras con el reportero de actina Lifeact etiquetado con GFP para seguir la dinámica de parches endocíticos y otras estructuras de actina de alto orden durante la regeneración de hifas y el re-establecimiento del crecimiento polarizado. Se estableció una línea de tiempo de la dinámica de las estructuras de actina de alto orden y se encontró que la remodelación de la pared celular y la membrana plasmática gracias a los parches endocíticos tiene un papel esencial en la regeneración de hifas. Adicionalmente, se visualizó a la proteína endocítica de cubierta temprana AP180 etiquetada con GFP y se observó que se localiza principalmente en el collar endocítico pero también en parches dispersos a lo largo de la hifa. Se observó el fenotipo de la cepa "knock out" Δ*ap180* que resulta letal para las ascosporas, y otra mutante que carece del dominio N-terminal ANTH (AP180$^{\Delta ANTH}$-GFP), la cual es incapaz de forman un collar. Y finalmente, se realizó inmunoprecipitación de AP180-GFP y se encontraron proteínas de unión a actina como posibles interactores. Sumados, los resultados revelan una interesante y nueva visión del collar endocítico, demostrando que es necesario para el reciclaje de membrana, un proceso que opera en tándem con la exocitosis para conseguir la morfogénesis y crecimiento polarizado tan característicos de los hongos filamentosos.

Palabras clave: *Neurospora crassa*, endocitosis, exocitosis, collar subapical, parches.

Abstract of the thesis presented **by Marisela Garduño-Rosales** as a partial requirement to obtain the Doctor of Science degree in Life Sciences with orientation in Microbiology.

Regulation of endocytosis in *Neurospora crassa* and its role in morphogenesis

Abstract approved by:

_____

Rosa Reyna Mouriño Pérez, DSc

Thesis Director

The present study examines fundamental aspects of endocytosis as a process involved in morphogenesis and polarized growth. We developed a photobleaching procedure based on FRAP (Fluorescence Recovery After Photobleaching) to measure endocytosis in hyphae of *Neurospora crassa* expressing the endocytic reporter fimbrin with a green fluorescent protein tag (FIM-1-GFP). We calculated that under standard growth conditions about 12.5% of the plasma membrane discharged in the apex becomes endocytosed in the subapex, with an average of occurrence of 21.4 endocytic events/min/μm^2 in an endocytic collar area of 236.7 μm^2. We conducted the FRAP procedure in hyphae grown in scarcity of nutrients and found an average occurrence of 30.4 endocytic events/min/μm^2 in an endocytic collar area of 79.1 μm^2. Additionally, we measured the internalization of the endocytic marker FM4-64 and found the same values of fluorescence intensity in both nutritional conditions. We followed conidial germination to assess the establishment of the endocytic collar using the strains FIM-1-GFP y FIM-1-mChFP/CHS-1-GFP (chitin synthase 1). We found that at the beginning endocytic patches form a cap at the very tip of the germling and once the germ tube reaches a length of ~150 µm, the arrangement of patches starts shifting to a subapical collar. Additionally, we performed mechanical injury experiments in mature hyphae with the actin reporter Lifeact tagged with GFP to follow the dynamics of endocytic patches and other high order actin structures during hyphal regeneration and re-establishment of polarized growth. We established a timeline of the dynamics of actin high order structures and found that remodeling of the cell wall and plasma membrane involving the endocytic patches plays an essential role in hyphal regeneration. Additionally, we visualized the early coat endocytic protein AP180 tagged with GFP and observed that it primarily localizes at the endocytic collar but also as scattered patches along the hypha. We observed the phenotype of the "knock out" mutant Δ*ap180* which is ascospore lethal, and another mutant lacking the N-terminal ANTH domain (AP180$^{\Delta ANTH}$-GFP) that is not able to form a collar. Finally, we immunoprecipitated AP180-GFP and found actin-binding proteins as possible interactors. Taken together our results reveal an interesting and novel insight to the endocytic collar, demonstrating that it is necessary for membrane recycling, a process that operates in tandem with exocytosis to attain hyphal morphogenesis and polarized growth.

Keywords: *Neurospora crassa*, endocytosis, exocytosis, subapical collar, patches.

Dedication

To my parents, Marisela y Sergio.

To my siblings, Karlita y Checo.

But mainly, to myself.

Acknowledgments

Thanks to the National Council for Science and Technology (CONACyT) for granting me the scholarship no. 299974.

Special thanks to the Center for Scientific Research and Higher Education of Ensenada (CICESE) for being my home during all these years and for all its support to complete my degree. Thanks to all the amazing people that make this place what it is.

I am very grateful for having the best advisor I could ever ask for, Dr. Rosa R. Mouriño Pérez. Thank you for all the guidance throughout these years, for the therapeutic laughs and encouragement words, for believing in me, for supporting my risky and crazy ideas, for your patience, for supporting me to go to all the possible meetings, for supporting me to go to the UK, for teaching me how to network, for teaching me that my happiness and well-being is more important than any degree, for being a great mentor and a friend, but also thank you for teaching me how to walk alone. Thank you for being you, you are truly amazing and inspiring, the toughest and most powerful woman scientist I know. I am the luckiest student in CICESE, without a doubt.

Special thanks to Dr. Salomon Bartnicki García, “god of the VSC”. You have had an impact in my career and life that I really cherish. I will always treasure the anecdotes, protips, advice and laugh you have shared with me. Thank you for teaching me how to question everything, it may not sound so good, but you know exactly what I mean. Thank you for all your support and for making me love fungal cell biology. I would not be here if it was not for you and Dr. Mouriño.

Special thanks to my dear friend, thesis committee member, and colleague Dr. Olga A. Callejas Negrete. Thank you for teaching me most of what I know in the lab, for teaching me how to make figures and for being there in the roughest times. Thank you for all the good times we have shared. You are one of the strongest female persons I know.

Special thanks to Dr. Brian D. Shaw, the best endocytosis buddy and thesis committee member in the world. Thank you for always giving me great advice and feedback, for receiving me in your home while I visited College Station, for sharing cool science, microscopy, jokes, drinks, and music.

Special thanks to Dr. Astrid Nalleli Espino Vázquez, whom I lucky to call my friend, besides being a great thesis committee member. Thank you for all the help and feedback, you might as well win an award as the most careful and critical reader of the thesis, and I am so grateful for that. You are one of the kindest

people I know. Thank you for all the laughs and dances, and for introducing me to Nef Cruz and Vero Garrido.

Thanks to all my labmates from Mouriño's group throughout these years: Tonancy, Abraham, Nahum, Rosita, Rocío, Ale, Alejandro, Gaby, Lara, Ariane, Ivan, Fausto, Yolanda, Alexia, Ricardo, Kevin, Paola, and many others that I am sure I am forgetting (I blame it on post-COVID brain fog). Thank you for being such great colleagues, meeting's partners, and many of you awesome friends. We are the most enthusiastic, joyful, and fun group.

Thanks to the Department of Microbiology. I cannot imagine being part of any other department in CICESE. We're the best! Thank you doctors: Gilberto, Ernestina, Meritxell, Rufina, Jimena, and Edgardo. Thanks for the many talks during "coffee breaks" to Juanito, Liz, Yael, Samantha, Juanpy, Luis Enrique I and II, Raquel, Pam, Anayatzin, Luis, Mena, Jenny, Alfredo, and many others.

Thanks to the National Laboratory for Advanced Microscopy in CICESE (LNMA-CICESE) and all its staff for the support with microscopy experiments. Special thanks to my good friend and colleague, the brilliant Dr. Diego L. Delgado Álvarez, who opened the endocytic path for me and is always up for cool science -and beer- talk.

Special thanks to all the amazing people that has supported me in the lab and paperwork. Guillermo Gonzalez, the best technician, and a good buddy. Adriana Mejía, who always saved me when it came to paperwork, money support, classes, etc., and has always been a kind friend to me. Really, this thesis would not be happening if it was not for you, Adri. Anabel Domínguez, who came and save our lives, thank you Anabel for being the very best at your job. Also, thanks to Amparo Valverde and Melissa Corral. Thanks to Miriam, Normita, Citlalli and Dolores for being great at your jobs. Thanks to Mrs. Lulis and Don Gustavo for always being kind and friendly to me.

Thanks to The Sainsbury Laboratory (TSL) for having me and letting me work there. Special thanks to Prof. Nick J. Talbot, who always made me feel as part of his group rather than just a visitor; thanks for all his support, meetings, guidance, invitations to write articles, and dance moves. I'm forever grateful to Dr. Lauren S. Ryder (SS) for teaching me lots of molecular biology while I was at TSL, for her patience, for being a great friend and karaoke partner, for her help with English and life in general! And thank you for still being there for me, you are the best. Also, thanks to -almost- Dr. Neftaly Cruz Mireles (BS), who is my thesis twin, my friend and fellow Mexican pursuing the British dream, thanks for all the support, for cheering me up, for teaching me proteomics and for helping me to survive in the UK. Thanks to Camilla Molinari, who welcomed me and was a great labmate and friend; thank you and Noemi for all the

croquetas, agua de Valencia, jokes, tattoos, dance flow, yummy biscuits, RPDR, and love. Also, thanks to Alice Eseola, Iris Eisermann, Weibin Ma, Xia Yan, Natalia Makarovsky, Cristina Molinero, Bozeng Tang, Andrew Deatker, Andy Foster, Diana Gómez, Juanca de la Concepción, Pablo del Cerro, Isa Diez, Liz Packham, Frank Menke, Paul Derbyshire, and Simon Foster.

Thanks to my dear friends and colleagues Dr. Oded Yarden and Dr. Inbal Herold for inviting me to collaborate with you and think outside the -hyphal tip- box. Also, I would like to thank my friends Dr. Blake Commer and Joe Vasselli for all the fun endocytosis talk. Thanks to my dear friends Monse Rentería and Isaí Acosta, you have been there for me, listening my complaints, concerns, a thousand deadlines, and even helping me study for my predoctoral exam; my heart always feels warm and full when I am with you. And thanks, in general, to all the great scientists I have met along the road.

Thanks to the Mycological Society of America (MSA) for honoring me with the 2018 “Francis A. Uecker” travel award to attend IMC11 in Puerto Rico, and for poster award. Thanks to the *Neurospora* Research Community for honoring me with the 2021 Perkin’s award. Thanks to the Mexican Society of Biochemistry (SMB) and the Molecular and Cellular Biology of Fungi section for oral presentation awards in 2017 and 2019 and granting scholarships to attend their meetings. Thanks to the Graduate Program Council of Life Sciences (CPP-CV) for supporting me financially to attend meetings and my research stay in the UK.

This thesis would not have been possible without the support of my family. Thank you, mom (Marisela Rosales), dad (Sergio Garduño), Checo (Sergio Garduño Jr.), and Karlita (Karla Garduño), for always believing in me, pages are not enough to express how grateful I am to call you, my family. Thank you being there for me always and unconditionally. Thank you for making me remember that I am a human and that I need to take care of myself above all things. Thank you for loving me and helping me become the person I am, for your patience and kindness. Thank you for growing with me and letting me grow with you. You are simply the best. Les amo con todo mi corazón.

Thanks to my amazing padrino (Jorge Garduño) and Oom (Kees de Haan), you have always believed and supported me. Thanks to the rest of my family, I deeply love you, but if I thank each one of you, I will never finish the “acknowledgments” section.

Thanks to my best -normal non-scientist- friends Fer Horta, Paula Nudelman, Leo Alemán, and Nera Ayala. Thank you for distracting me off science and making me feel appreciated and love. It feels good talking other things apart from nerdy stuff. Thanks to all my other friends, you are forever in my heart. I am forever grateful for having the best therapist in the world, Dr. Noemí Gutiérrez, thank you for all the guidance and giving me tools to take care of myself.

Thanks to all the amazing people I have met along this road, I am sure I must be forgetting some names, please do not take it personal.

And last, but not least, I want to thank my “past” self, for making the choices to bring me where I am now, for loving biology, and having a great curiosity.

Table of contents

List of figures

List of tables

Chapter 1. Introduction

1.1 Background

Filamentous fungi, like yeast, are excellent models for studying eukaryotic cells, as in general terms, they have fast growth rates, are easy to cultivate, and live-cell observations have been successfully standardized for various types of microscopy. Filamentous fungi have a high polarized apical mode of growth, similar to pollen tubes and root hairs in plants, and neurons in mammals. Their basic physiological structure is a cylindrical cell known as hypha. Many hyphae together are called mycelium. Filamentous fungi can grow and colonize a great variety of substrates because of the apical growth and lateral branching capability. For polarized growth to be optimal, a highly active secretory machine is required to keep a good number of secretory vesicles arriving to thehyphal apex. These vesicles are exocytosed from the apical dome in a gradient, and they deliver enzymes in charge to expand the membrane and build more cell wall (Bartnicki-García, 2002). The VSC (Vesicles Supply Center) is the essence of a mathematic model, showing that hyphal shape is achieved by a gradient of secretory vesicles (Gierz and Bartnicki-Garcia, 2001). The cloud of vesicles at hyphal tips, called the Spitzenkörper acts as a VSC, i.e. the supply center of vesicles (Grove and Bracker, 1970; López-Franco and Bracker, 1996). This has been the paradigm to understand hyphal growth, and it has focused on exocytosis mediated by the Spitzenkörper (Bartnicki-García, 2002; Girbardt, 1969; Harris et al., 2005; Riquelme and Bartnicki-García, 2008; Sánchez-León et al., 2011; Steinberg, 2007; Trinci, 1969). It has been proposed that the insertion of new membrane by secretory vesicle fusion causes an excess in the apical plasma membrane relative to the quantity of cell wall components required to maintain an effective tip extension (Read and Hickey, 2001). Recent research has pointed out that **a balance between exocytosis and endocytosis** is important for fungal morphogenesis (Schultzhaus and Shaw, 2015).

Neurospora crassa is one of the most studied filamentous fungi, due to its sequenced and well anotated genome that facilitates genetically manipulation to study cellular processes, metabolic pathways, and proteins specific functions, among others. The existence of endocytosis in filamentous fungi has been questioned (Cole et al., 1998). Specifically, it was suggested that endocytosis in *N. crassa* did not exist (Torralba and Heath, 2002). However, several studies suggest otherwise, as it has been widely demonstrated that endocytosis does not only occur in *N. crassa* and other filamentous fungi, but it is an essential process to hyphal morphogenesis (Araujo-Bazán et al., 2008; Atkinson et al., 2002; Delgado-Álvarez et al., 2010; Echauri-Espinosa et al., 2012; Fuchs et al., 2006; Hernández-González et al., 2018;

Lara-Rojas et al., 2016; Peñalva, 2005, 2010; Read and Kalkman, 2003; Schultzhaus et al., 2017; Schultzhaus and Shaw, 2015; Shaw et al., 2011). Authors have mentioned that the presence of homologs of endocytosis genes (from *Saccharomyces cerevisiae*) in filamentous fungi may be considered bona fide evidence for the functional conservation of endocytosis (Wendland and Walther, 2005). Actin cytoskeleton is known to participate in all types of endocytosis. Nonetheless, knowledge about endocytosis is very limited in filamentous fungi.

The actin network is constantly remodeling to participate in diverse critical processes, such as endocytosis, exocytosis, cytokinesis, cell polarity, and cellular morphogenesis. It is believed that these events are possible due to the coordinate action of a set of 20-30 highly conserved proteins associated with actin, and many other proteins specific to each cell, as well as several upstream signaling molecules (Moseley and Goode, 2006). The combined activity of these factors orchestrates with precision the spatial and temporal assembly of the actin structures, and it ensures the dynamic turnover of actin structures so cells can rapidly alter their cytoskeletons in response to external and internal cues. The machinery and mechanisms that control the assembly of the different actin structures are highly conserved (Moseley and Goode, 2006). The main high order structures of actin are cables, contractile actomyosin rings, and patches. Each of these are associated to an actin-dependent process (Adams et al., 1991; Arai et al., 1998; Berepiki et al., 2010; Bretscher, 2003; Delgado-Álvarez et al., 2014; Delgado-Álvarez et al., 2010; Moseley and Goode, 2006; Pruyne and Bretscher, 2000; Roberson, 1992; Sandrock et al., 1999; Schultzhaus and Shaw, 2015; Taheri-Talesh et al., 2008; Upadhyay and Shaw, 2008).

Actin patches are composed of multiple proteins associated with actin, and characterization experiments of patch composition in yeast *S. cerevisiae* (e.g. actin, Arc35, Rsv167, Sac6, and Vrp1) have demonstrated that the main defects are related to endocytosis. Therefore, the mutants of these proteins have been collectively termed *end* mutants (Chvatchko et al., 1986; Dulic and Riezman, 1989; Engqvist-Goldstein and Drubin, 2003; Kubler and Riezman, 1993; Moseley and Goode, 2006; Munn et al., 1995; Raths et al., 1993; Riezman, 1985). An internalization deficiency of the dye Lucifer Yellow was detected in yeast cells treated with anti-actin drug Latrunculin A, which established the link between actin to endocytosis (Ayscough et al., 1997; Moseley and Goode, 2006). Components of endocytic patches have been labeled with the green fluorescent protein (GFP), and it has been observed that patches are very dynamic (Delgado-Álvarez et al., 2010; Doyle and Botstein, 1996; Echauri-Espinosa et al., 2012; Lara-Rojas et al., 2016; Waddle et al., 1996). It seems that actin patches mature in states according to stages of endocytosis, and they are characterized by possessing different types of movement (Moseley and Goode, 2006).

Some proteins function as coats for endocytic vesicles to assist them in the transport of certain molecules. Also, they support vesicles formation and maintenance of their integrity and specificity. These coat proteins are formed around nascent vesicles (Schultzhaus et al., 2017). The most studied type of endocytosis is the one mediated by the coat protein complex **clathrin**. The clathrin complex is composed of two proteins, the "heavy" (Chc1) and "light" (Clc1) chains, which form a structure similar to a triskelion with three copies of each subunit. When these structures bind, they form a reticulum around the sites where membrane invaginates to provide structural support for membrane bending through the natural curvature of the reticulum and to help vesicles fission (Brodsky, 1988; Brodsky et al., 2001; Kukulski and Picco, 2016; Schultzhaus et al., 2017). Two phases are recognized in yeast endocytosis. The early phase has a variable duration, 60-180 s, in which cargo congregates in "nascent" sites, and clathrin coats establish around invagination. The late phase has an approximate duration of 35 s, where actin nucleation promotes invagination, and vesicle scission and its distancing from plasma membrane occur (Kukulski et al., 2012; Kukulski et al., 2011; Schultzhaus and Shaw, 2015; Weinberg and Drubin, 2012). At least 60 proteins are involved in clathrin-mediated endocytosis (CME) (Moseley and Goode, 2006). The following endocytic modules with protein of similar dynamics in each of them have been proposed: early arriving proteins, coat, WASp/MYO, amphiphysins, actin and scission (Kaksonen et al., 2005; Lu et al., 2016; Moseley and Goode, 2006; Weinberg and Drubin, 2012). The coat module is subdivided in early, intermediate and late (Lu et al., 2016; Moseley and Goode, 2006; Weinberg and Drubin, 2012). A scheme of the clathrin-mediated endocytosis can be observed in **¡Error! No se encuentra el origen de la referencia.**.

Although endocytosis is a very conserved process in general, in *Aspergillus nidulans*, it was observed that the main site of localization of clathrin was not to the endocytic collar (Schultzhaus et al., 2017). These results strongly suggest that despite being necessary for the fungus viability, clathrin is not involved in the endocytosis occurring at the subapical collar.

Studying endocytosis is especially interesting in filamentous fungi, because in the subapical zone of hyphae there is a collar (of ~9 µm long in *N. crassa*) made of patches that contain endocytic proteins such as actin, fimbrin, coronin, arp2/3, myosin 1, among other, where endocytosis is enriched (Delgado-Álvarez et al., 2010; Echauri-Espinosa et al., 2012; Lara-Rojas et al., 2016; Schultzhaus et al., 2016; Taheri-Talesh et al., 2008; Upadhyay and Shaw, 2008). When the expression of any of these proteins is compromised, the cell is not fully capable of internalizing the dye FM4-64 (known to be uptaked via endocytosis) and hyphal morphogenesis is severely affected (Delgado-Álvarez et al., 2010; Echauri-Espinosa et al., 2012; Lara-Rojas et al., 2016). FM4-64 internalization has been proven to be energy, temperature, and F-actin dependent, which suggests that it occurs by endocytosis (Yamashita and May, 1998).

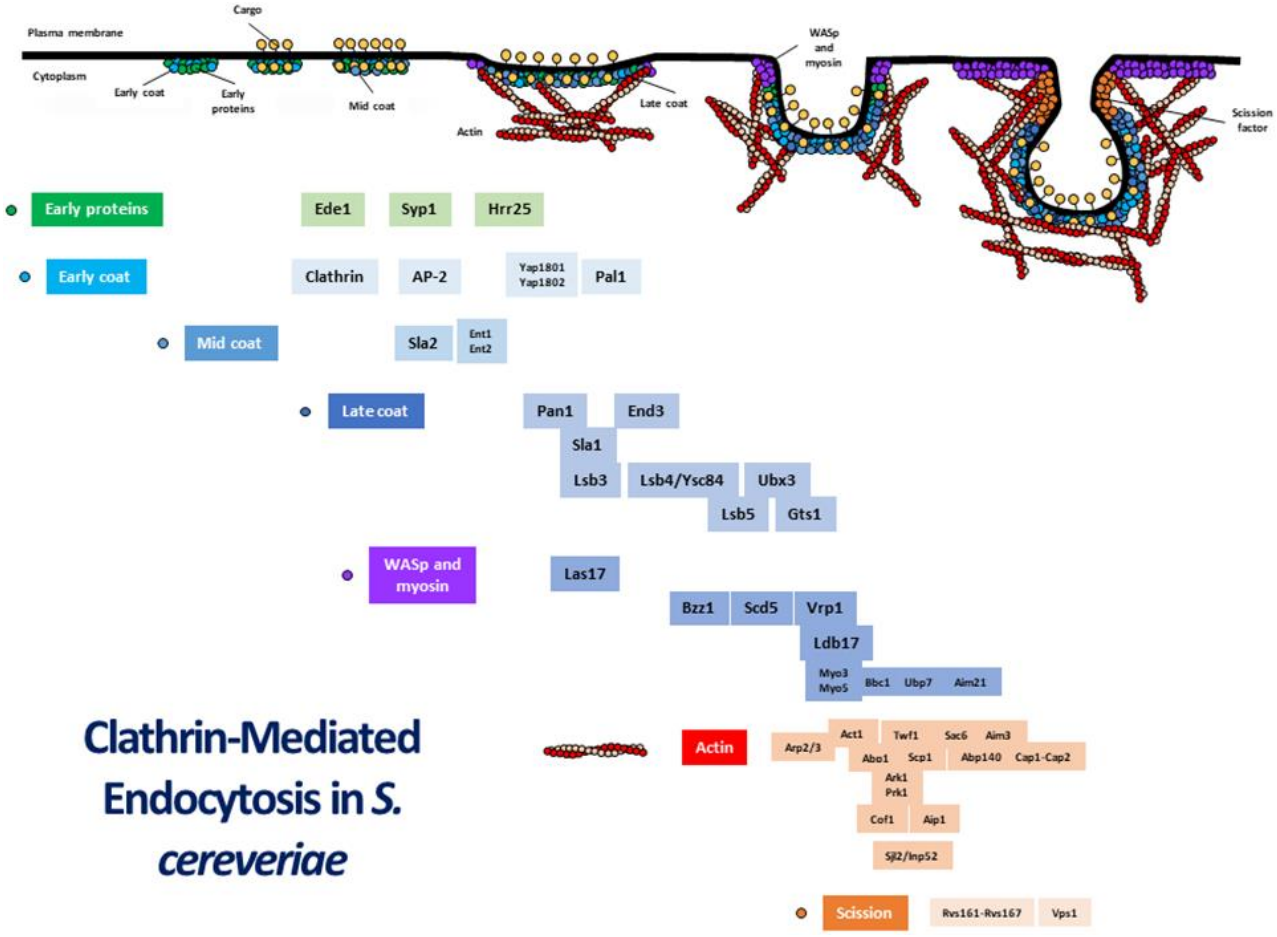

Figure 1. Clathrin-Mediated Endocytosis in *Saccharomyces cerevisiae*. CME is divided in different modules as we can observe in this scheme: 1) Early proteins, 2) early coat, 3) mid coat, 4) late coat, 5) WASp and myosin, 6) actin, and 7) scission. The modules are represented by the action of specific proteins, although some of the modules occur almost simultaneously. The lifetime of the endocytic proteins is highly variable among them. Clathrin appears in the early coat module. This schematic cartoon is modified from Lu et al. (2016).

It has been suggested that in the subapical collar is where membrane excess produced by secretion is recovered. In addition to its important role in membrane recycling, endocytosis has been proposed to play a fundamental part in the recycling of the polarization machinery at the apex, by preventing its diffusion and displacement in the Apical Recycling Model (Shaw et al., 2011). Moreover, even though the precise details are very poorly understood, it is evident that this highly specialized endocytic zone has an essential role in hyphal morphogenesis.

The mechanisms behind site selection in clathrin-mediated endocytosis (CME) are still poorly understood (Brach et al., 2014; Lu and Drubin, 2017; Lu et al., 2016; Stimpson et al., 2009; Weinberg and Drubin, 2012). In *S. cerevisiae* the first proteins to arrive to endocytic site have an important role in cargo capture and

efficiency of site initiation (Brach et al., 2014; Lu and Drubin, 2017). However, the mechanism for site initiation is highly flexible, which was demonstrated in mutants of early phase proteins that are dispensable for vesicle formation and internalization, although they are necessary for regulated recruitment of cargoes (Brach et al., 2014; Lu and Drubin, 2017). Adaptor proteins selectively recognize and bind cargoes, lipids, and coat proteins and anchor the forming coat to plasma membrane (Maldonado-Baez et al., 2008; Reider and Wendland, 2011). For adaptor proteins to concentrate cargo, they must cluster at the endocytic site, and this seems to rely on a great number of weak protein-protein interactions between the adaptors (AP180, AP-2), cargoes, clathrin, and the early endocytic protein Ede1 (Maldonado-Baez et al., 2008). Experiments have demonstrated that the minimal requirements for the initial stage of coated pit invagination are clathrin, AP180, AP-2, and PtdIns(4,5)P_2-containing membranes (Ford et al., 2001). The proteins that act in the endocytic site selection and coat maturation have not been identified in filamentous fungi, but looking into the homologs of yeast can provide useful leads.

AP180 is an important multifunctional component of the early coat of endocytic vesicles (Morris et al., 1993). It possesses a N-terminal ANTH domain, followed by several DxF motifs which bind to AP-2 adaptor appendages. Also, it contains a central clathrin interaction site. The ANTH domain is conserved from human to yeast; it binds to phosphatidylinositol-4,5-biphosphate [PtdIns(4,5)P_2] via a lysine-rich interaction site. As AP180 binds to PtdIns(4,5)P_2 and clathrin simultaneously, it is thought to tether clathrin to the membrane (Ford et al., 2001). AP180 has been shown to interact *in vitro* with clathrin triskelia and promote their assembly into 70-80 nm cage-like structures (Ahle and Ungewickell, 1986). In *S. cerevisiae*, two homologs of human AP180 have been identified: Yap1801 and Yap1802 (Wendland and Emr, 1998).

To determine the percentage of the plasma membrane excess removed in *N. crassa* by endocytosis, we developed a fluorescence recovery after photobleaching (FRAP) procedure and a calculation sheet to process our measurements. We wanted to explore the effect of the scarcity of nutrients in hyphal growth and endocytosis, and using our FRAP procedure we found out that there seem to be more endocytic events in hyphae growing in low nutrient medium than in standard medium. To further explore this outcome, we performed FM4-64 internalization experiments with a laser scanning confocal microscopy (LSCM) and saw no difference between the dye internalization between the fungi grown in the two media. To unravel the ontogeny of the endocytic collar, we utilized endocytic reporters tags and LSCM in germlings. To assess the role of the actin endocytic patches and other actin cytoskeleton structures during hyphal regeneration, we performed mycelial mechanical injury and followed the regeneration process with LSCM. To describe the localization and dynamics of the early arriving endocytic coat protein AP180, we performed LSCM, Spinning-Disk Confocal Microscopy (SDCM), and Total Internal Reflection Fluorescence Microscopy

(TIRFM). To determine if AP180 is important for *N. crassa* development, we observed the phenotype of two different mutants of *ap180*. And last, to identify putative interactors of AP180, we performed immunoprecipitation and mass spectrometry of AP180-GFP.

1.2 Project justification

It is crucial to describe the characteristics of the endocytosis as a physiological phenomenon to understand the morphogenesis and polarized growth of filamentous fungi. Endocytosis is a special process in these fungi, that is highly concentrated in the subapical region, immediately behind the apical growth region.

The study of the endocytosis in these organisms is relatively new. Some fundamental questions remain unanswered, such as: 1) under what conditions is excess membrane generated via exocytosis so endocytocis can take place? 2) when is that the endocytic collar establishes at the hyphal subapex? 3) does membrane remodeling only occur in healthy hyphae? and 4) is there a clathrin-independent pathway that regulates the endocytosis occurring at the subapical collar?

1.3 Hypothesis

- The endocytic rate is lower when there is a decrease of hyphal growth
- The endocytic collar establishes once the germ tube reaches a critical growth speed.
- Endocytic patches contribute to the re-initiation of hyphal polarized growth following mechanical injury.
- The so-called clathrin adaptor AP180 is an early coat protein in *N. crassa* that acts in a clathrin-independent manner.

1.4 Goals

1.4.1 General goal

Decipher the function, genesis, and regulation of the subapical endocytic collar in the filamentous fungus *N. crassa*.

1.4.1 Specific goals

1. Establish the ratio between endocytosis and exocytosis.

2. Evaluate the effect of nutrient stress on the endocytic rate.

3. Establish the ontogeny of the endocytic collar.

4. Visualize the actin endocytic patches and other actin cytoskeleton structures dynamics for polar growth recovery after mechanical injury.

5. Visualize the localization and dynamics of the early coat endocytic protein AP180.

Chapter 2. Methodology

2.1 Strains and culture conditions

Strains used in this study are listed in Table 1**¡Error! No se encuentra el origen de la referencia.**. Strains were maintained on Vogel's minimal medium (VMM) with 1.5% sucrose. All manipulations were carried on according to standard techniques (Davis, 2000).

Table 1. Strains of *Neurospora crassa* used in this study.

Strains	Genotype, description, or sequence	Reference
Wild-type 2225	*mat A*	FGSC2225
Wild-type 2489	*mat a*	FGSC2489
9717	*mat A his-3⁻; Δmus-51::bar⁺*	FGSC9717
TRM08-DD02 (FIM-1-GFP)	*mat a his-3⁺::Pccg-1-fim-1-sgfp⁺*	Delgado-Álvarez et al., 2010
TRM-DD06 (FIM-1-mChFP)	*mat A his-3⁺::Pccg-1-fim-1-mcherryfp⁺*	Lara-Rojas et al., 2016
NES2-11	*mat A chs-1::sgfp⁺::hph⁺*	Sánchez-León et al., 2011
NJV12.1.1	*mat A his-3⁺::Pccg-1-chs-1-mcherryfp⁺*	Verdin et al., 2009
TRM-MG01 (FIM-1-mChFP/CHS-1-GFP)	*het a his-3⁺::Pccg-1-fim-1-mcherryfp⁺/chs-1::sgfp⁺::hph⁺*	This study
CLC-mCHFP	*het A his-3⁺::Pccg-1-clc-1-mcherryfp⁺*	Lara-Rojas, unpublished
AP180-GFP	*mat a ap180-sgfp⁺::hph⁺*	Lara-Rojas, unpublished
AP180$^{\Delta ANTH}$-GFP	*mat A his-3⁺::Pccg-1-ap180$^{\Delta C}$-sgfp⁺*	Lara-Rojas, unpublished
FGSC19506	*mat a Δap180::hph⁺*	Colot et al., 2006

2.2 Experimental measurement of the endocytosis/exocytosis ratio in mature hyphae

FRAP (Fluorescence Recovery After Photobleaching) experiments were performed on growing tips of mature hyphae expressing the FIM-1-GFP tag with a laser scanning confocal microscope (LSCM). Mycelium was grown for 12-18 h at 30^{o}C and an agar block from the border of the colony was cut and mounted onto

a coverslip and incubated at RT for 30 min to allow recovery. Images were recorded with the focal plane set closest to the plasma membrane. To quantitate endocytosis, the number of endocytic patches appearing in the following frame after photobleaching in an area of 25 μm^2 (5 X 5 µm) were counted. DIC images were simultaneously recorded to determine hyphal diameter and elongation rates, parameters that were used to calculate the area of exocytosed plasma membrane. By doing so, it was possible to estimate an exocytosis/endocytosis rate.

2.3 Growth rate

To estimate the differences in the growth rate of mycelium subjected to nutritional stress in comparison to normal nutrient quantity, we inoculated mycelial disks of 8 mm containing the FIM-1-GFP strain onto a margin of plates of VMM with different quantity of nutrients (Table 2) by quintupled. Instead of agar as a gelling agent we used molecular grade agarose for greater purity. We incubated the cultures in total darkness at 25^{o}C. We made the first measurement at 10 hpi (hours post -inoculation) and proceed to do follow up measurements every 4 h until a total time of 26 h was covered. We analyzed the date with Fiji and Microsoft Excel.

Table 2. Culture media used on growth rate estimations and experiments of nutrient stress conditions.

Culture medium	% Vogel's salts 50X	% Saccharose	% Agarose
Vogel's minimal medium 100%	2	1.5	1.5
Vogel's minimal medium 50%	1	0.75	1.5
Vogel's minimal medium 0% (water agarose)	0	0	1.5

For further experiments we decided to use VMM 100% and VMM 0%, from now on referred as VMM and WA, respectively.

2.4 Measurement of endocytosis under nutrient stress condition

The ratio between endocytosis and exocytosis in scarcity of nutrients was measured in the strain tagged with FIM-1-GFP grown in WA using the FRAP quantification method previously. Additionally, we measured

FM4-64 internalization, for which we inoculated VMM and WA (both containing agarose instead of agar) with 9mm mycelial disks of FIM-1-GFP. About 18 hpi we mounted samples for laser-scanning confocal microscopy using the inverted-agar block method (Hickey et al., 2002) and let them rest for an hour before observing. Once the samples were visualized and the hyphae looked fully recovered and healthy, we added a small volume of FM4-64 7.5 µM endocytic marker with an insulin syringe in the margin of the agar block to observe the dye internalization. Images were captured with a delay of 1 min between each frame to avoid photobleaching. Time lapsed image sequences were analyzed in Fiji to measure fluorescence intensity. The fluorescence intensity was measured at 0, 3, 6 and 9 minutes after FM4-64 injection, and it was specifically measured at the 10 µm behind the apex (Echauri-Espinosa et al., 2012). Data was collected, normalized, and graphed in Microsoft Excel. A total of 44 hyphae were observed for VMM and 68 for WA.

2.5 Generation of FIM-1-mCHFP/CHS-1-GFP strain

We generated a mat A heterokaryon strain expressing both FIM-1-CHFP (endocytic marker) and CHS-1-GFP (exocytic marker), by promoting mycelial fusion of the strains by inoculating them in close proximity in VMM. We screened the strain with LSCM looking for both fluorescent signals. We made three follow up cultures to ensure the obtention of the heterokaryon strain and then promote conidiophore production in Erlenmeyer flasks with 50 ml of VMM to harvest conidia.

2.6 Ontogeny of the endocytic collar

N. crassa strain tagged with FIM-1-GFP and a heterokaryon strain co-expressing FIM-1-mCHFP and CHS-1-GFP were used to follow the ontogeny of the endocytic collar, using two methodologies.

1) Conidia of FIM-1-GFP were cultured in VMM 1.5% and observed by confocal microscopy (as described in the Live-cell imaging section). Observations were conducted every hour after germ tube emergence until the endocytic collar was established.

2) Diluted suspensions of the heterokaryon strain were prepared ($1x10^6$ conidia ml^{-1}). We placed 10 µl of the conidia suspension onto a coverslip and then added a clean VMM agar block over it. We let the samples

sit for 15 min and then observed by laser-scanning confocal microscopy. Images were captured with a delay of 15 min between each frame to avoid photobleaching and stressing the sample. Also, we added little cotton pieces soaked in liquid VMM at the margins of the agar block to slow down agar desiccation. Germination was followed for up to 9 h.

2.7 Assays of mechanical injury of mature hyphae

Mycelia of Lifeact-GFP and CHS-1-mChFP tagged strains were cut with a scalpel close to the colony margin to analyze the regeneration of the injured hyphae. Once the sample was visualized on bright field microscopy, we performed mycelial injury, and a time-lapse was recorded using LSCM (see Live-cell imaging section) to follow the behavior of F-actin in hyphal compartments that were immediately anterior to the injury site. We followed this process for 2-3 h.

2.8 Assays of F-actin and microtubules depolymerization following mechanical injury of mature hyphe

To study the effect of cytoskeleton depolymerization on hyphal regeneration, mycelia of Lifeact-GFP tagged strain were separately injected with the anti-actin drug latrunculin B (Lat B) at 20 µg ml^{-1} and the anti-microtubules drug benomyl (Ben) at 2.5 µg ml^{-1} (Sigma-Aldrich, St. Louis, MO) immediately after the injury (Ramos-Garcia et al., 2009). Observations were carried out for 2-3 h.

2.9 Visualization of the localization and dynamics of AP180

Subcellular localization and dynamics of the early coat protein AP180 in mature hyphae were attained using LSCM, SDCM and TIRFM. FM4-64 dye was added to observe membranous organelles. Detailed methodology of the microscopy can be found below in the Live-cell imaging section.

2.10 AP180 mutant characterization

Germinating ascospores of the “knock-out” mutant of AP180 were imaged by confocal microscopy using the cell wall stain calcofluor white to assess phenotype.

Additionally, a mutant of AP180 lacking the N-terminus ANTH domain was analyzed. The mutant is C-terminally tagged with GFP. Elongation rate was measure in a laser scanning confocal microscope, using also the FM4-64 dye to observe membranous organelles.

2.11 Live-cell imaging

Strains containing fluorescent markers were being grown on VMM for 12 h at 30 ^{o}C. The “inverted agar block” method (Hickey et al., 2002) was used for live-cell imaging with spinning-disk confocal, laser scanning confocal and total internal reflection fluorescence microscopes.

Inverted microscope Eclipse Ti-U (Nikon, Japan) is equipped with a spinning-disk module CSU-X1 (Yokogawa, Japan) and a camera iXon Ultra (Andor, UK) for confocal microscopy (SDCM), which allow to capture multiple points of light simultaneously to excitation, offering high temporal resolution. Furthermore, this microscope is also equipped with an illumination module Ti-LAPP and a camera Orca Flash 4.0 (Hamamatsu, Japan) for total internal reflection fluorescence microscopy (TIRFM). Laser lines for excitation in this microscope include 405, 488, 561 and 640 nm. Apo TIRF 60x and 100x, (NA 1.49) oil immersion objectives will be used in both types of microscopy. Time-lapse images were captured by fluorescent channels with NIS-Elements Advanced Research software (Nikon, Japan).

Inverted laser scanning confocal microscope (LSCM) FV1000 FluoView^{TM} (Olympus, Japan) is equipped with a Multi-line Ar laser for excitation at 488 nm for GFP and a He-Ne(G) laser for excitation at 543 nm for mCHFP. An UPlanFLN 60x, (NA 1.42) oil immersion objective was used. Time-lapse images will be captured simultaneously by fluorescent and DIC (Differential Interference Contrast) channels with FluoView^{TM} software (Olympus, Japan).

Final images and videos are being created with Adobe Photoshop CC 2017 (Adobe Systems Inc., San Jose, CA) and Camtasia Studio 8 (TechSmith Corp., Meridian, MI).

2.12 AP180-GFP immunoprecipitation (IP) experiments and liquid chromatography tandem mass spectometry (LC-MS/MS) analysis

IP experiments and peptide preparation for LC-MS/MS were based on Bozkurt et al. (2011) and Petre et al. (2015) with some modifications. We set up liquid cultures of cytosolic GFP (cyto-GFP) and AP180-GFP strains in Complete Media (CM; see Appendix) by triplicate and incubated at 30 ^{o}C, 150 rpm in total darkness. After 24h, we harvested the mycelia with dH_2O, filtered with miracloth using a funnel and collecting everything in a bottle. We poured filtered mycelia in 50 ml centrifuge tubes pre-chilled with liquid nitrogen, then placed the frozen samples in the freeze dryer for 2 days and stored in -80 ^{o}C until they were processed.

For protein extraction, we resuspended each freeze-dried sample in extraction buffer [GTEN (glycerol 10%, Tris pH 7.5 25 mM, EDTA 1mM, NaCl 150mM), PVPP 2%, DTT 10 mM, 1x protease inhibitor cocktail (Sigma, Burlington, MA), IGEPAL 0.1%, phosphatase inhibitor tablet (1 tablet per 50 ml)] and then transferred to a pre-chilled 2 ml microcentrifuge tube containing a metal ball. We grinded the samples using Geno-grinder at 1 min/1500 rpm, and then centrifuged at 4 ^{o}C at maximum speed for 10 min. We transferred the supernatant to a 5 ml pre-chilled centrifuge tube and resuspended pellet in extraction buffer. We calculated protein concentration by Bradford assay and used 25 µg to do a Western Blot to confirm, input was even.

We added GFP-Trap beads (ChromoTek, Germany) and IP buffer (GTEN, 0.1% Tween) to the protein extracts and left the IP samples rotating for 3 h using a rotor in a cold room, then washed samples with IP buffer 5x and centrifuged at 800 rpm for 1 min. We removed the supernatant and washed with IP buffer, and then removed the buffer. We eluted immunoprecipitated proteins in loading buffer at 70 ^{o}C in a Thermomixer, and then centrifuged at 800 rpm for 1 min. We loaded 5µl of each sample in a precast gel for SDS-PAGE analysis.

For IP-MS, we took the leftover of the sample and loaded it into a new precast gel, ran the samples until they entered 1 cm in the gel (~15 min at 90 V). Then, cut each sample/well individually in six gel pieces and put them into 2 ml Protein LoBind tubes (Eppendorf, Germany). We performed in gel digestion of the samples with trypsin to extract peptides. LC-MS/MS data processing and protein identification were performed as described by Zess et al. (2019). For IP-MS proteome analysis we used the database *Neurospora crassa* (strain ATCC 24698 / 74-OR23-1A / CBS 708.71 / DSM 1257 / FGSC 987).

To determine what proteins were potential interactors of AP180, we summed spectral counts from the three experiments. Summed counts for AP180-GFP were then divided by the summed counts for cyto-GFP to give a ratio. We added 1 to the value of all cells. So, if 10 counts were observed this became 11. If zero counts observed the value was 1. This was done to derive a ratio (bait protein vs control) for all proteins identified, then to convert to log2 and rank high-to-low. Any values 2-fold greater or more in AP180 compared to cyto-GFP were considered as possible interactors. Anything less than 2-fold or lower in AP180 compared to cyto-GFP was discarded. Anything in between was considered as non-differential.

Chapter 3. Results

3.1 Establish the ratio between endocytosis and exocytosis

3.1.1 Experimental measurement of the ratio between endocytosis and exocytosis in mature hyphae

To quantify the frequency of endocytic events, FRAP experiments were conducted on hyphae of *N. crassa* tagged with FIM-1-GFP. Individual hyphae were selected for evidence of normal growth, Spitzenkörper presence, regular morphology, and stable fluorescence. Hyphal tips were examined by focusing on the upper cortex close to the plasma membrane where actin cables and actin patches are localized (Delgado-Álvarez et al., 2010).

Table 3. FRAP experiment to estimate membrane internalized by endocytosis. A total of 60 hyphae of *Neurospora crassa* tagged with FIM-1-GFP were analyzed.

	Average	**Media**	**Standard Error**
Exocytosis (by geometry)			
Growth rate (µm/min)	6.7	6.2	0.5
Hyphal diameter (µm)	8.4	8.3	0.2
Exocytic vesicle diameter (µm)*		0.08	
Exocytic vesicle surface (μm^2)		0.02	
Exocytosed membrane (μm^2/min)	179.9	169.2	9.7
Endocytosis			
Endocytic collar length (µm)*		9.0	
Endocytic collar area (μm^2)	236.7	234.2	3.7
Endocytic vesicle diameter (µm)*		0.04	
Endocytic vesicle surface (μm^2)		0.005	
FRAP experiments			
Endocytic events/min/μm^2	21.4	20.3	1.2
Total endocytic events in the collar/min	5,129	4,799	602
Endocytosed membrane (μm^2/min)	25.8	24.1	1.5
Percentage of endocytosed membrane %	12.5	14.2	1.8

** Endocytic collar length and vesicle diameter were considered constant throughout.*

The entire process was recorded, analyzing the frames before, during and after photobleaching (Figure 2).

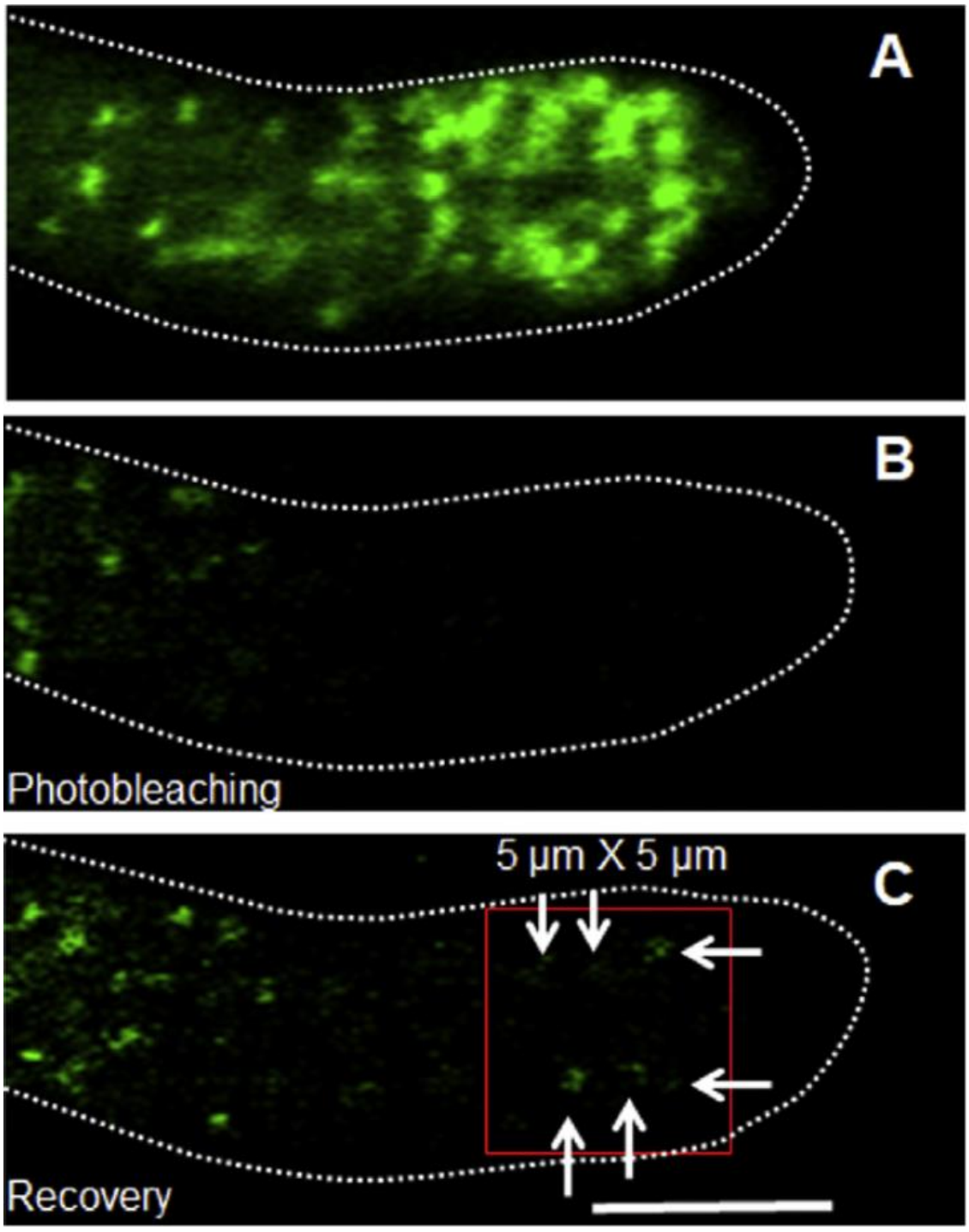

Figure 2. Stages in FRAP experiment to count endocytic events in a mature hypha of *Neurospora crassa* labeled with FIM-1-GFP. (A) Single plane confocal image of the endocytic collar of a hypha immediately prior to photobleaching. (B) 6 sec later. (C) Recovery after 2 sec (square shows area of new endocytic events counted). Scale bar = 5 µm.

Following bleaching of the collar, new fluorescent patches were counted, they varied in intensity but were all counted. Simultaneous calculations were made of the amount of plasma membrane generated from measurements of hyphal elongation. The amount of membrane endocytosed was calculated by assuming that each fluorescent patch internalized a vesicle of 0.04 µm in diameter. An examination of 60 hyphae revealed an average of 5,129 endocytic events in the collar per min (Table 3). This corresponds to 25.8 $\mu m^2\, min^{-1}$ of plasma membrane internalized in hyphae growing at 6.7 ± 0.05 µm min^{-1}. We calculated that the amount of endocytosed membrane was 12.5% of the total of plasma membrane generated by exocytosis.

3.2 Evaluate the effect of nutrient stress on the endocytic rate

3.2.1 Growth rate estimate in different nutrient conditions

To measure the difference in growth rate when decreasing nutrients, we evaluated three media: VMM 100%, VMM 50%, and VMM 0%. There was a growth reduction of only 17.06% in VMM 50% and of 42.46% in VMM 0% in comparison with VMM 100%, showing no significant difference between VMM 100% and 50% (Figure 3), for which we decided to only use the VMM (VMM 100%) and WA (VMM 0%) conditions to obtain and compare their ratio between endocytosis and exocytosis.

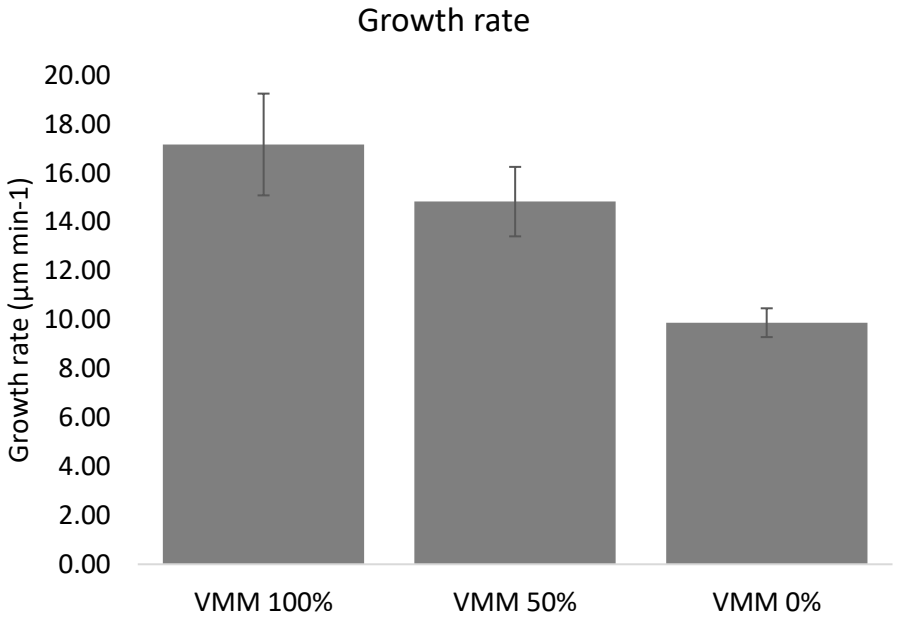

Figure 3. Comparison of hyphal growth rate among Vogel's derived nutrient-decreasing culture media. Plot shows no significant difference between VMM 100% (17.17±2.08 µm min^{-1}; average±95% confidence interval) and 50% (14.83±1.42 µm min^{-1}).

3.2.2 Experimental measurement of the ratio between endocytosis and exocytosis in mature hyphae with slow growth

To measure endocytosis in a condition of slow growth, we performed the FRAP procedure in hyphae grown in WA (Figure 4).

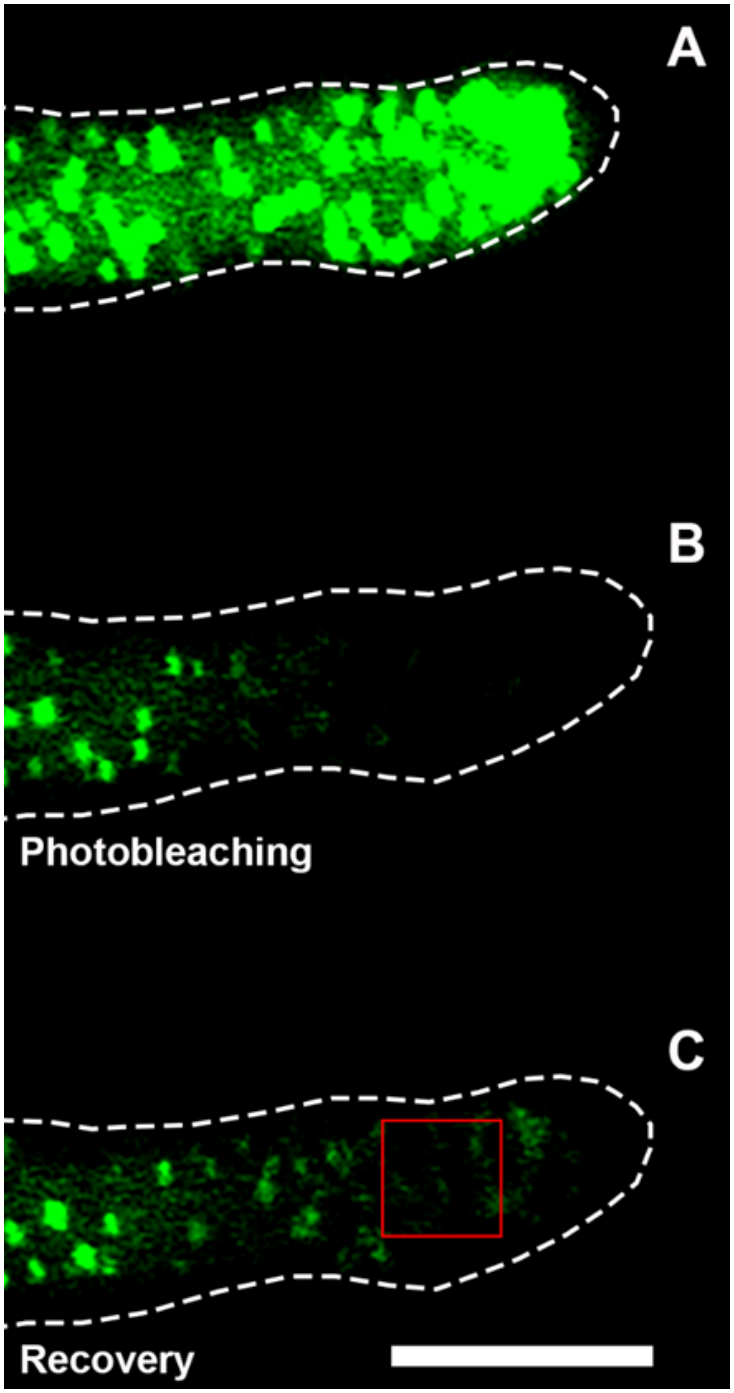

Figure 4. Stages in FRAP experiments to count endocytic events in a mature hypha of *Neurospora crassa* labeled with FIM-1-GFP and grown in Water Agar. (A) Single plane confocal images of the endocytic collar of a hypha immediately prior to photobleaching. (B) 6 sec later. (C) Recovery after 2 sec (square shows area of new endocytic events counted). Scale bar = 10 μm.

Data are summarized in Table 4. In our observations, there is a clear increase in the number of endocytic events in time and surface in the hyphae grown in WA, with a value of 30.4±4.2 (average±standard error) endocytic events $min^{-1}/\mu m^2$, while in the VMM the value was 21.4±1.2 endocytic events $min^{-1}/\mu m^2$ (n_{WA}=18 hyphae; n_{VMM}=60 hyphae). By contrast, the elongation rate was 6.7±0.5 µm min^{-1} vs 1.1±0.2 µm min^{-1}, VMM and WA respectively (Figure 5).

Additionally, we found that the length of the endocytic collar in the WA condition is ~4.7 µm, which is shorter than the ~9 µm reported by Delgado-Álvarez et al. (2010) in VMM.

Table 4. FRAP experiment to estimate membrane internalized by endocytosis. A total of 18 hyphae of *Neurospora crassa* tagged with FIM-1-GFP grown in WA (water agar) were analyzed. Average±standard error.

EXOCYTOSIS (by geometry)	*WA*
Growth rate (µm/min)	1.1±0.2
Hyphal diameter (µm)	5.4±0.2
Exocytosed membrane (μm^2/min)	17.9±3.1
ENDOCYTOSIS	
Endocytic collar length (µm)	4.7
Endocytic collar area (μm^2)	79.1±2.3
Endocytic vesicle diameter (µm)*	0.04
Endocytic vesicle area (μm^2)	0.005
FRAP EXPERIMENTS	
Endocytic events /min/μm^2	30.4±4.2
Total endocytic events in the collar /min	2375.7±326.9
Endocytosed membrane (μm^2/min)	11.9±1.6
Percentage of endocytosed membrane %	94.6±17.5

** Endocytic collar length and vesicle diameter were considered constant throughout.*

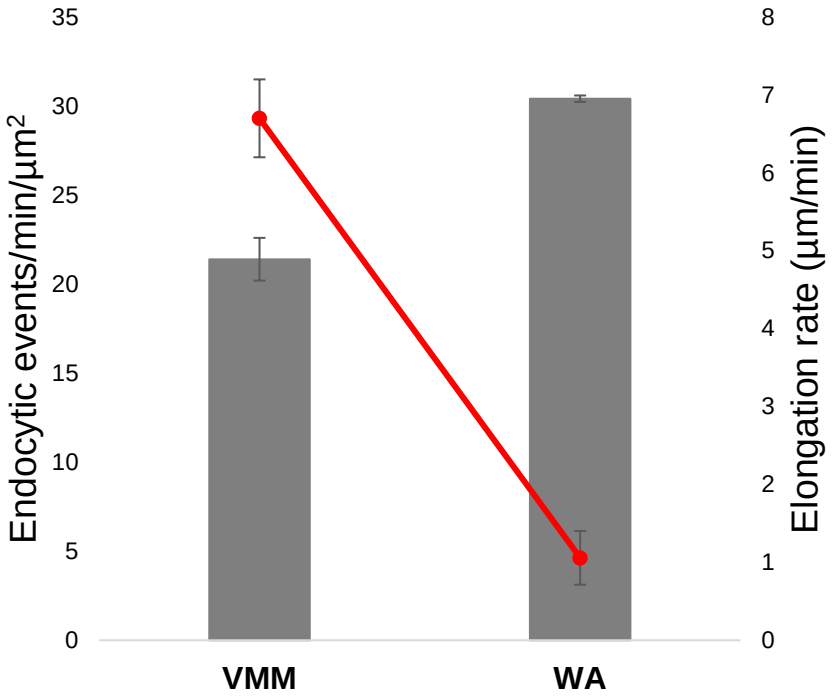

Figure 5. Comparison of endocytic events/min/µm2 and elongation rate between VMM and WA. Bars indicate the endocytic event and the red line the elongation rate (µm/min). Error bars correspond to standard error.

3.2.3 Internalization rates of the endocytic marker FM4-64

To further evaluate endocytosis under scarcity of nutrient we used the dye FM4-64 which is only internalized via endocytosis (Figure 6).

Once the sample was injected with the dye the whole plasma membrane was stained and it was possible to observe how it further stained the interior of the hyphae (including the Spitzenkörper and endosomes) as the time progressed in both conditions.

During our observations and following analysis, fluorescence intensity was the same for hyphae grown in VMM and WA.

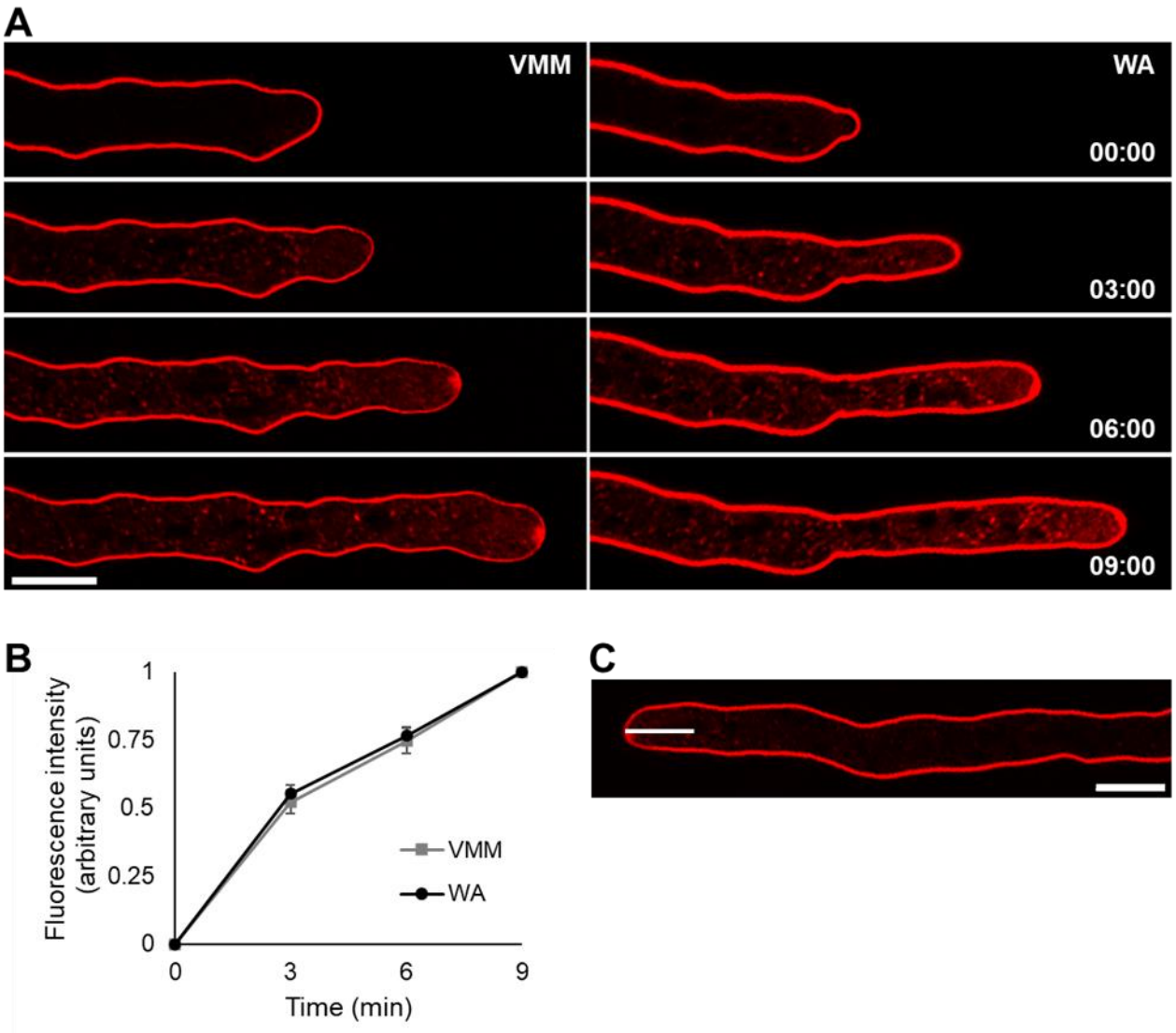

Figure 6. Comparative rates of internalization of the endocytic marker FM4-64 in mature hyphae of *Neurospora crassa*. (A) Hyphae grown in VMM and WA (B) Graph of fluorescence intensity in a subapical cytoplasmic region (10 µm from the tip) in VMM (n=44) and WA (n=68). (C) Shows the line where fluorescence intensity was measured. Time=mm:ss. Scale bars=10 µm.

3.3 Establish the ontogeny of the endocytic collar

Using the strain FIM-1-GFP we followed conidia germination and observed by laser scanning confocal microscopy the establishment of the endocytic collar (Figure 7). It was found that the patches are localized throughout the plasma membrane in conidia and they concentrate where the germ tube emerges; then they accumulate mainly in the tips in a cap-like fashion, although patches are visible also in the subapical region (**¡Error! No se encuentra el origen de la referencia.**8). We observed that when the tube reaches

the length of ~150 µm and an elongation rate ≥0.5 µm min^{-1}, the patches started localizing conspicuously and mainly in the subapex (**¡Error! No se encuentra el origen de la referencia.**9). Also, we noticed that at the first stages of germination, tube elongation was exponential and somewhere around the 400 µm of tube length the elongation becomes linear (Figure 10).

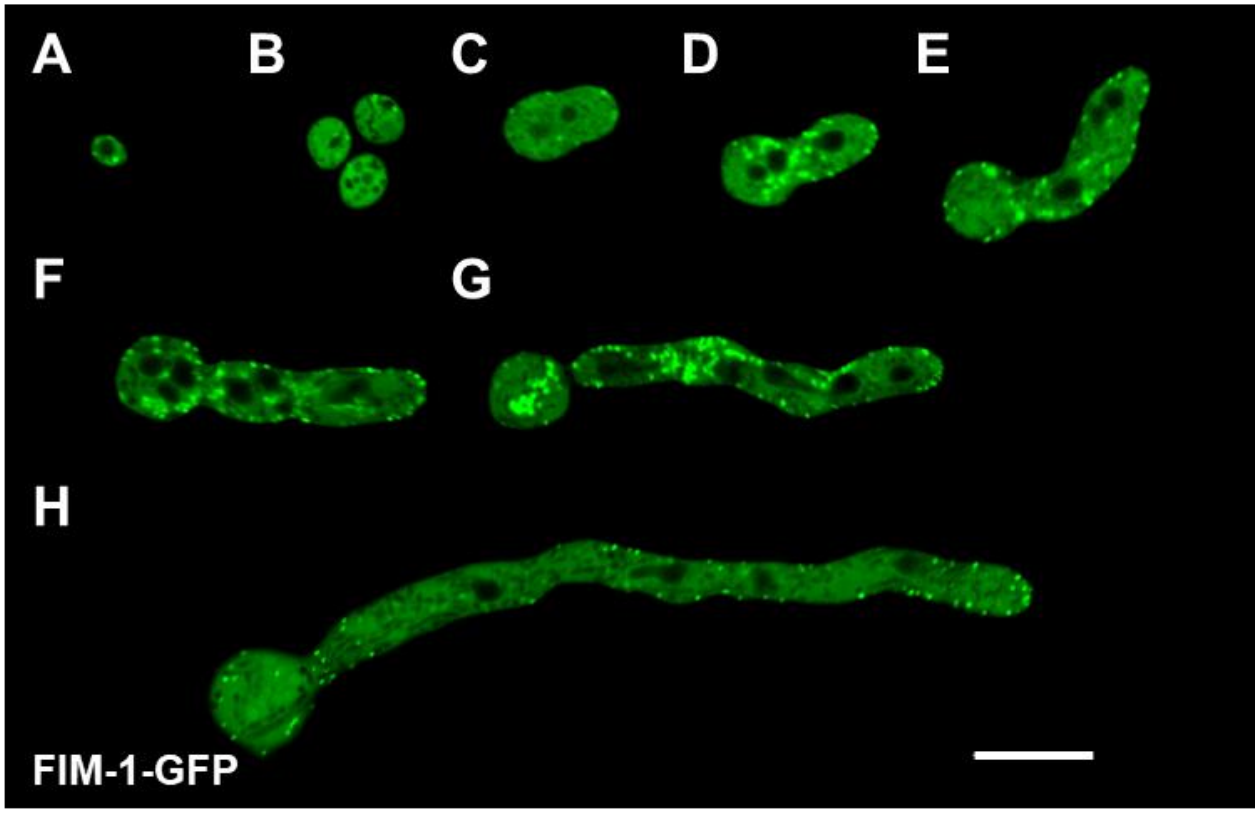

Figure 7. FIM-1-GFP localization during germination in *Neurospora crassa*. (A-B) Patches localize throughout the plasma membrane in conidia. (C-E) Patches concentrate on the site of the tube emergence. (F-H) As the tube grows, a cap made of patches is noticeable in the apex. Other patches are visible along the tube. Scale bar=10 µm.

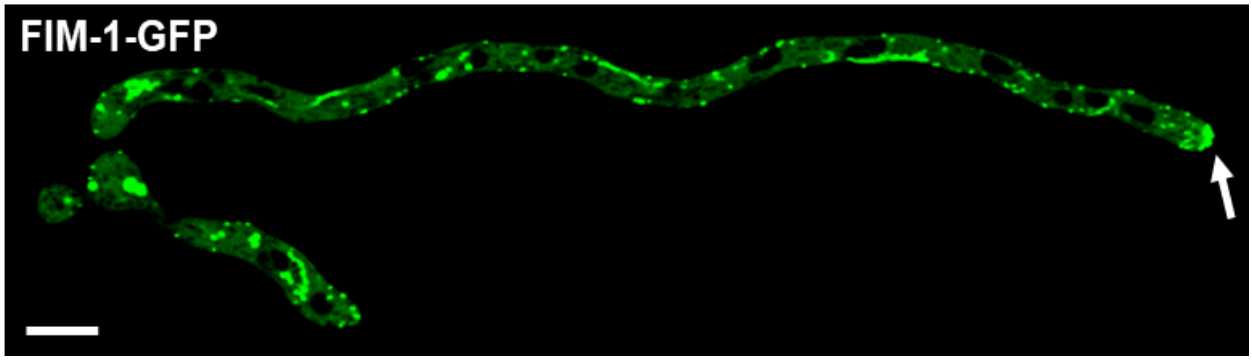

Figure 8. Germling of *Neurospora crassa* tagged with FIM-1-GFP. Arrow points at the cap. Scale bar=10 µm.

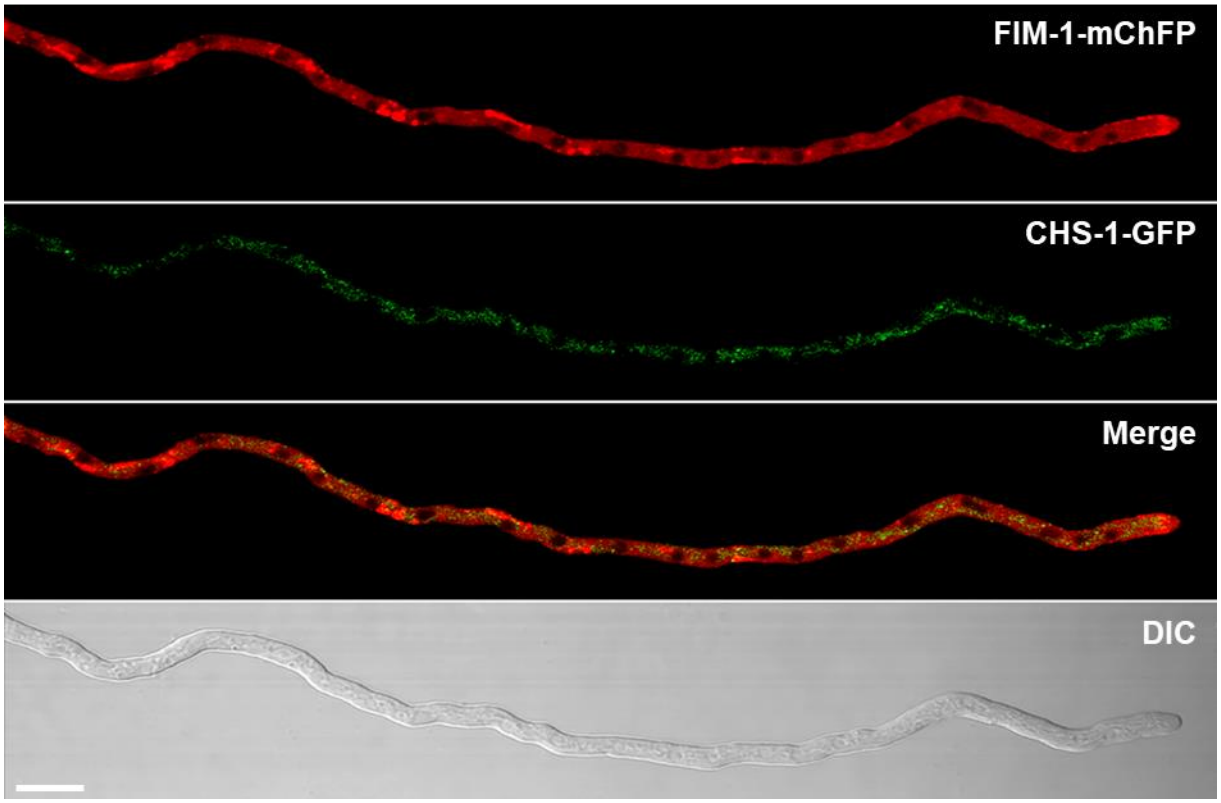

Figure 9. Heterokaryon strain of *Neurospora crassa* expressing FIM-1-mCHFP and CHS-1-GFP localization in a ~300 µm long germling. Arrow shows the endocytic collar already positioned at hyphal subapex. Scale bar=10 µm.

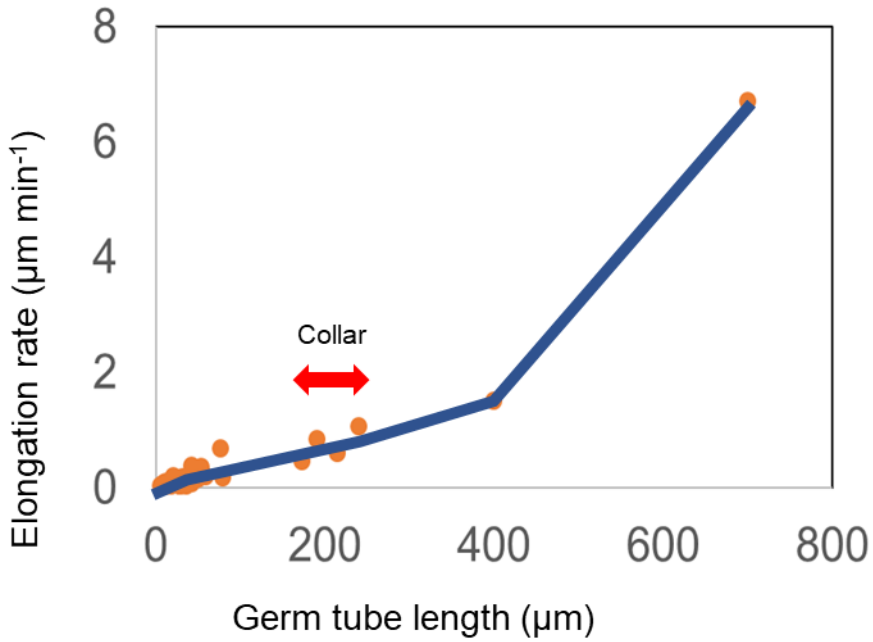

Figure 10. Germ tube length vs elongation rate. The endocytic collar establishes when the germ tube length is about 150 µm in *Neurospora crassa*. After that the elongation rate shifts from exponential to linear.

3.4 Visualize the actin endocytic patches and other actin cytoskeleton structures dynamics for polar growth recovery after mechanical injury

3.4.1 Actin dynamics following mechanical injury

Injuring of the mycelium of *N. crassa* with a scalpel caused immediate loss of cytoplasm in the hyphal compartments that receive the cut but not in the adjacent hyphal segments, whose septa became instantly plugged preventing further loss (Figure 11A). The surviving hyphae became extensively vacuolated.

F-actin accumulations were evident immediately after the cut (Figure 11B). Numerous long actin cables were visible radiating from the plugged septa, as well as actin patches accumulating in that zone to form a crescent-shaped dome (Figures 12 and 13). Once the new tip emerged from the plugged septum, the actin crescent differentiated into an actin cap. Newly regenerated hyphae grew within the damaged hypha from the plugged pore toward the adjacent empty hyphal segment; in some cases, two new hyphae were observed growing in the same empty compartment (Figure 12A and B). Within the first 30 min after mechanical injury, there was growth recovery in 17 of the 19 hyphae observed. There were new septation events in injured hyphae before new hyphae emerged (Figure 13A) with a consistent simultaneous correlation between septum formation and hyphal regeneration. The actin cap re-organized for the re-establishment of the tip growth apparatus, composed by two differentiated structures: the Spitzenkörper and the endocytic collar. This differentiation was observed within the first hour after the cut (Figure 13C).

We observed that the Woronin body was left aside as the new tips emerged from the plugged septa (Figure 14). We observed one event where two septa were plugged in the same hypha adjacent to the cut site (Figure 15). The new tip emerged from the plugged septum that was farther from the damaged site (Figure 15). Once the new tip reached the second plugged septum, it was unable to surpass it. We also observed a new septum development where the original plugged septum was and from where the new tip emerged (Figure 15).

We measured the hyphal elongation rate before and after injury. In regenerating hyphae, we started measuring the elongation rate once the new tips emerged. Hyphae showed an elongation rate of 7.1±0.3 $\mu m\ min^{-1}$ (mean±standard error) under normal growth conditions, whereas regenerating hyphae grew at 1.7±0.3 $\mu m\ min^{-1}$. The elongation rate of the new hyphae when compared to uninjured hyphae had a reduction of 76.1%. Additionally, we measured the diameter of the injured hyphae and the regenerated

hyphae that emerged from them. We found a reduction in the diameter of regenerated hyphae when compared to injured hyphae (carcasses) of 41.2%.

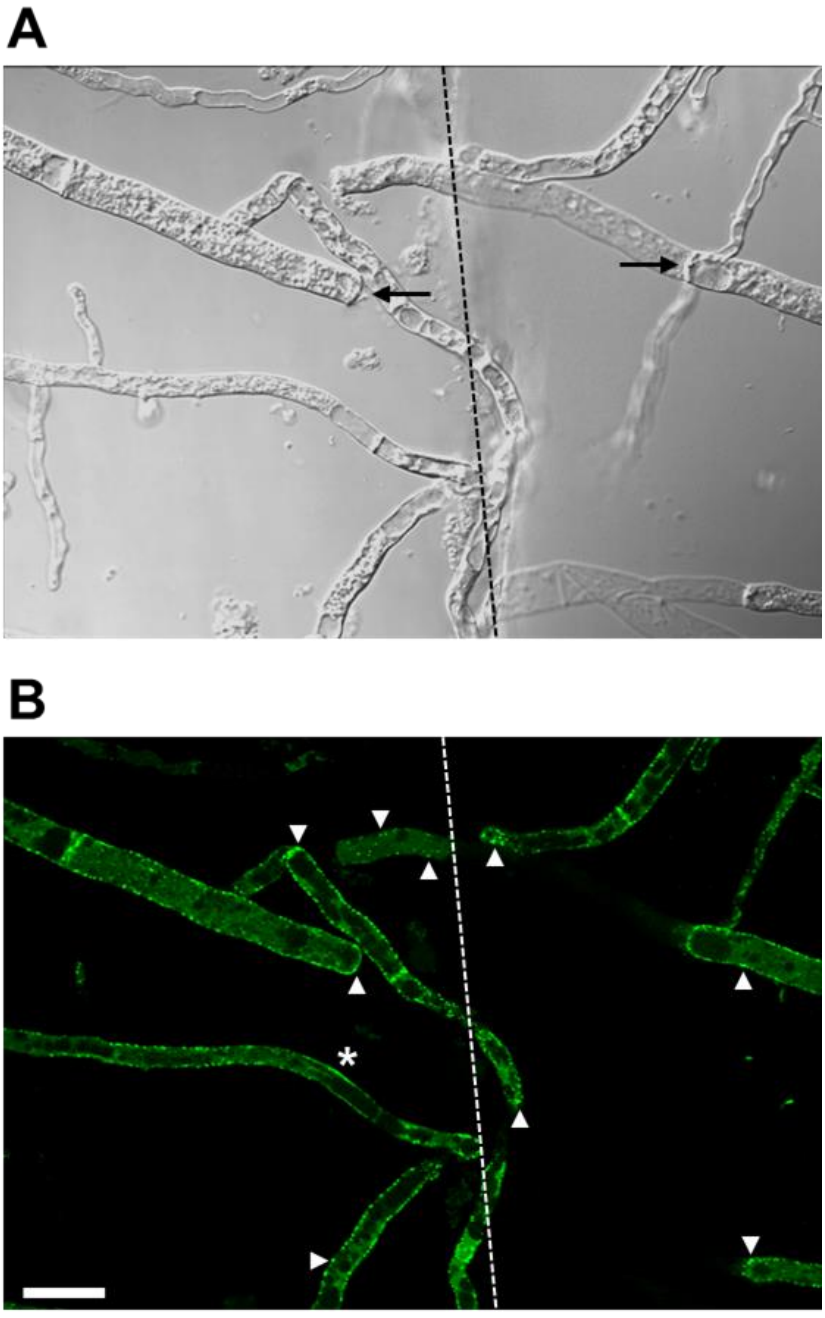

Figure 11. Immediate effects of mechanical injury on hyphae of *Neurospora crassa*. Fungus shows stressed hyphae with extensive vacuolation. (A) Dotted lines depict the site where the cut was made, and arrows point to the (plugged) septa that prevented a total loss of cytoplasm. (B) Lifeact-GFP image immediately after the cut, showing endocytic patches dispersed throughout the cell periphery. Arrowheads point to patches and asterisk to cables. Scale bar=20 µm.

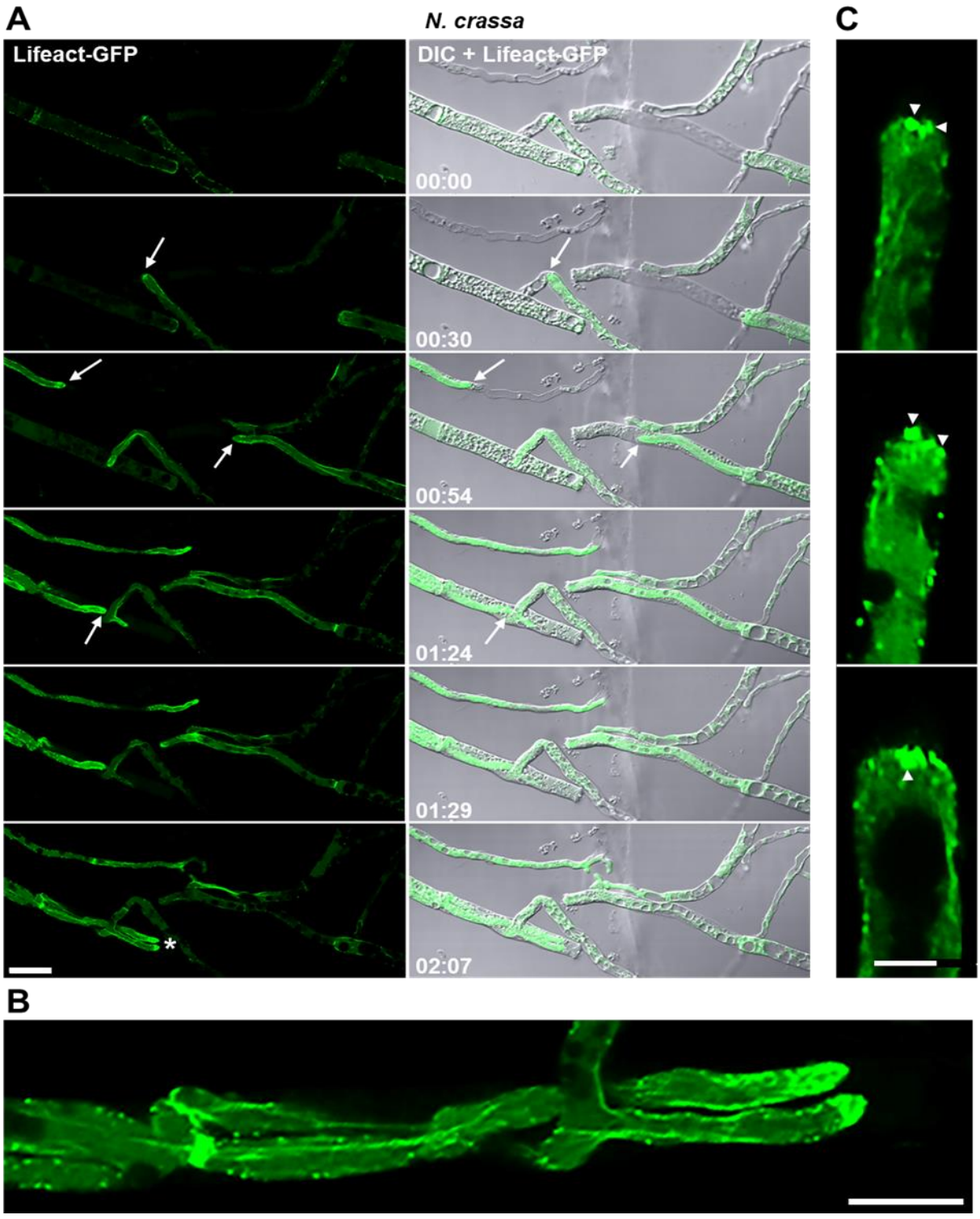

Figure 12. Actin dynamics after mechanical injury in *Neurospora crassa*. (A) Time-lapse shows the regeneration of hyphae. Arrows point to new growing hyphae and asterisk to two hyphae growing inside the same injured plugged hyphal compartment. High accumulations of actin (crescent) are visible as part of the re-shaping of the new tip from the plugged septum at ~30 min post-injury. The Spitzenkörper and the endocytic collar become visible once the hyphae re-start apical growth (Time 00:54). (B) Zoom-in shows the two new tips growing inside the plugged compartment. Scale bars=10 µm. (C) Actin patches accumulating at plugged septa close to the injury sites (arrowheads). Scale bar=5 µm. Time=hh:mm.

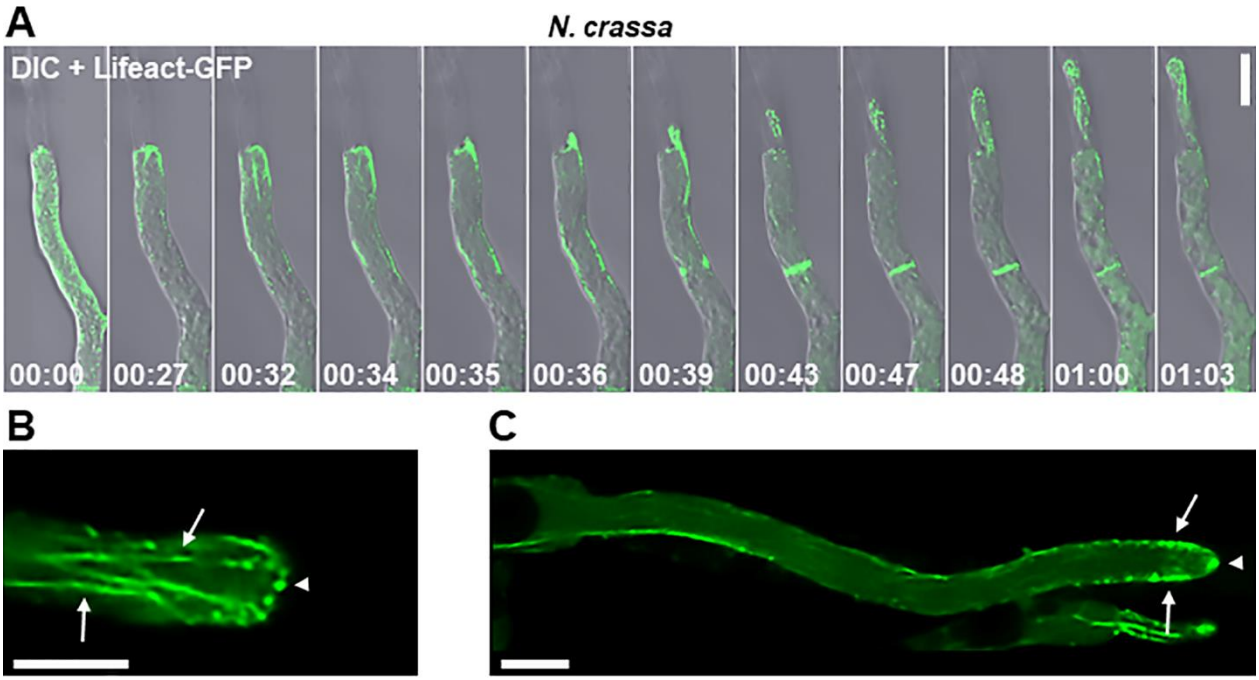

Figure 13. Actin dynamics during regeneration after mechanical injury in *Neurospora crassa*. (A) Time-lapse shows septum-development and emergence of a new hypha. (B) Long actin cables and patches are visible close to the plugged septa. (C) Re-established tip growth apparatus (arrowhead points to the Spitzenkörper and arrows to the endocytic collar) in a regenerated hypha. Scale bar=10 µm. Time=hh:mm.

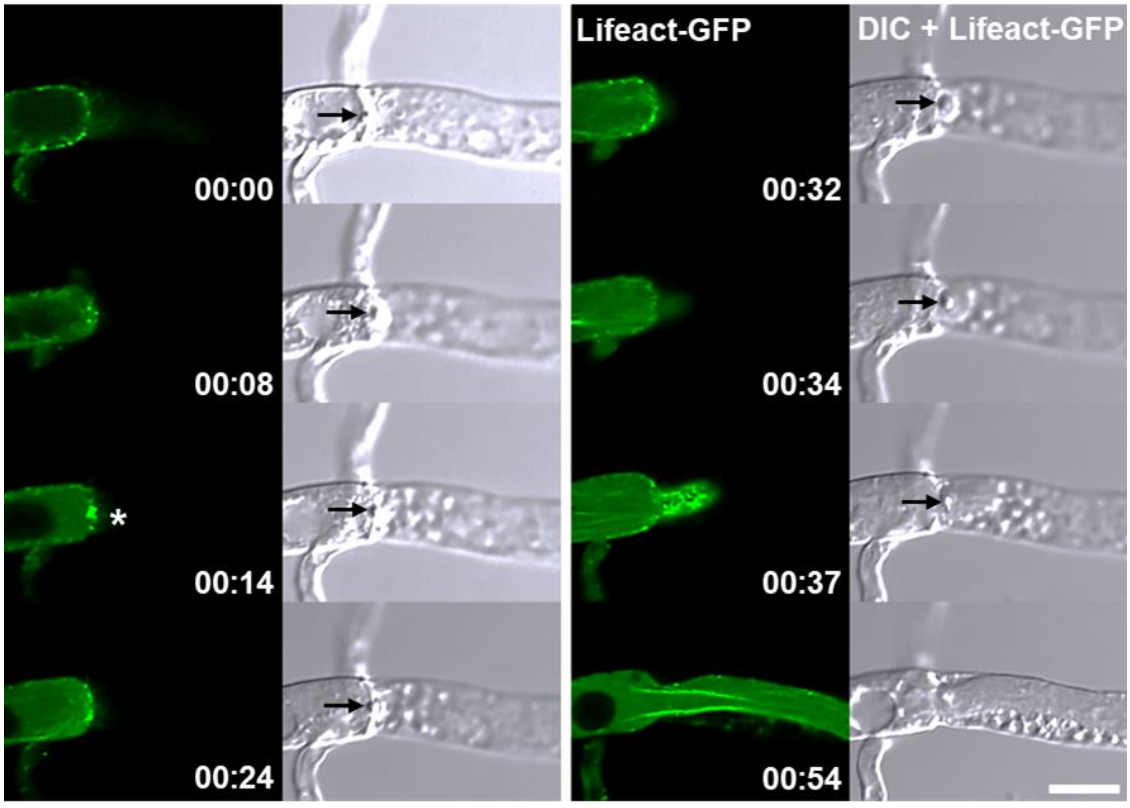

Figure 14. New tip emergence after mechanical injury in *Neurospora crassa*. Time-lapse shows tip emergence, where arrows point to the Woronin body throughout the whole process, and asterisk to actin patch accumulation. Scale bar=10 µm. Time=hh:mm.

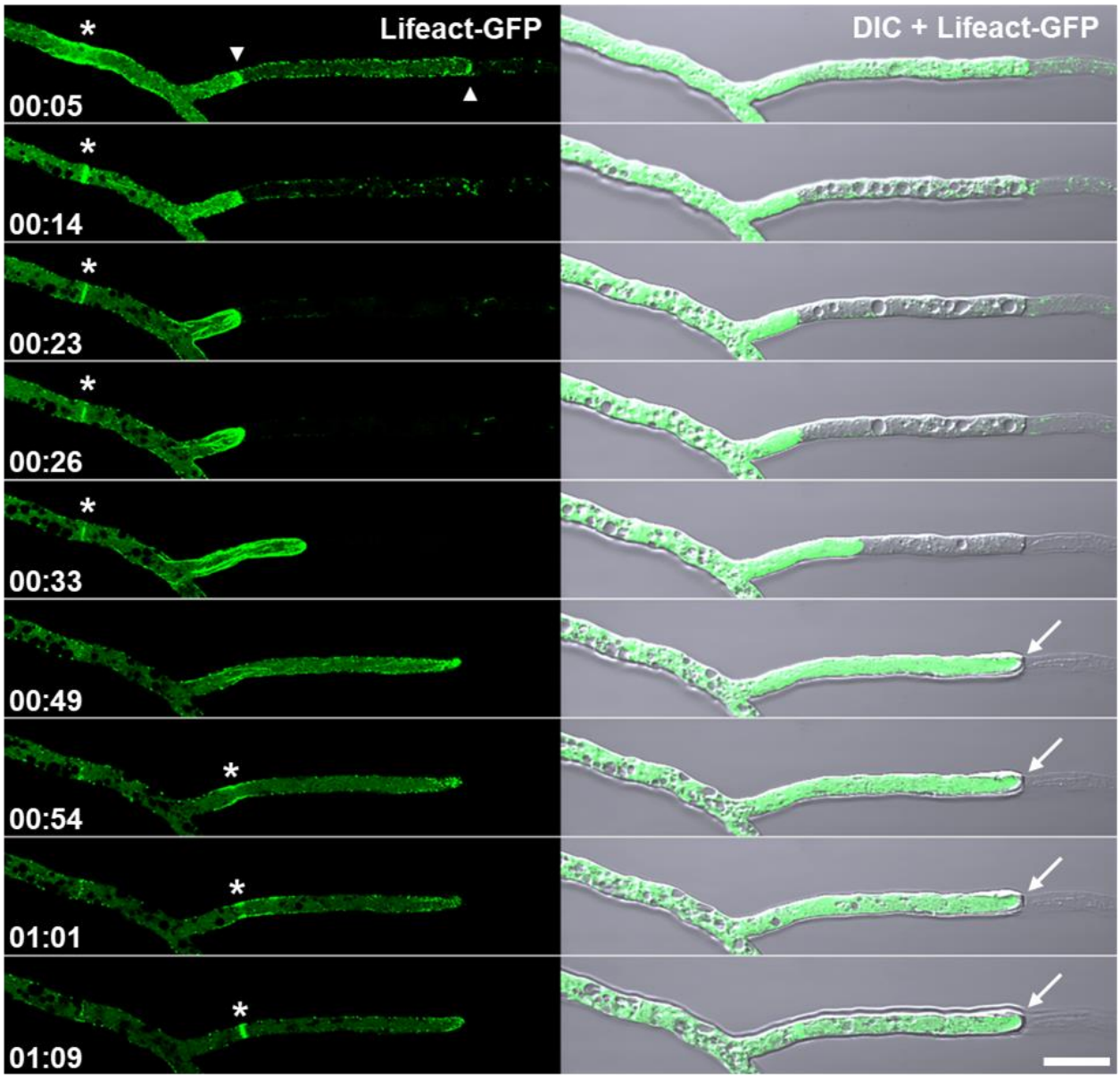

Figure 15. Two septa plugged by Woronin bodies in a same hyphal compartment in *Neurospora crassa*. Time-lapse shows an injured hypha with two plugged septa (arrowheads). Tip emerges from the further away plugged septum (from cutting site) and it reaches the second plug (Time 00:49; arrow) but it is unable to surpass it (Time 01:09; arrow). Asterisks point to septum development at the exact same site where there was the plugged septum from which the new tip emerged. Scale bar=10 µm. Time=hh:mm.

F-actin dynamics in mechanically injured mycelia treated with anti-cytoskeleton drugs as also visualized (Figure 16). The utilization of Lat B (anti-actin drug) resulted in stationary patches and total absence of cables. Actin patches did not accumulate immediately after mechanical injury instead they were visible ~30 min after injury and drug injection. Hyphal regeneration was severely affected as tip emergence from

the plugged septa was rarely achieved and maintained, ergo, polarized growth was not attained. It was common to observe the emergence of new lateral tips ~2:20 h after the injury, which went through an isotropic growth period and then resumed polarized growth (Figure 16). Benomyl (anti-microtubule drug) addition did not prevent hyphal regeneration and tip emergence after mechanical injury.

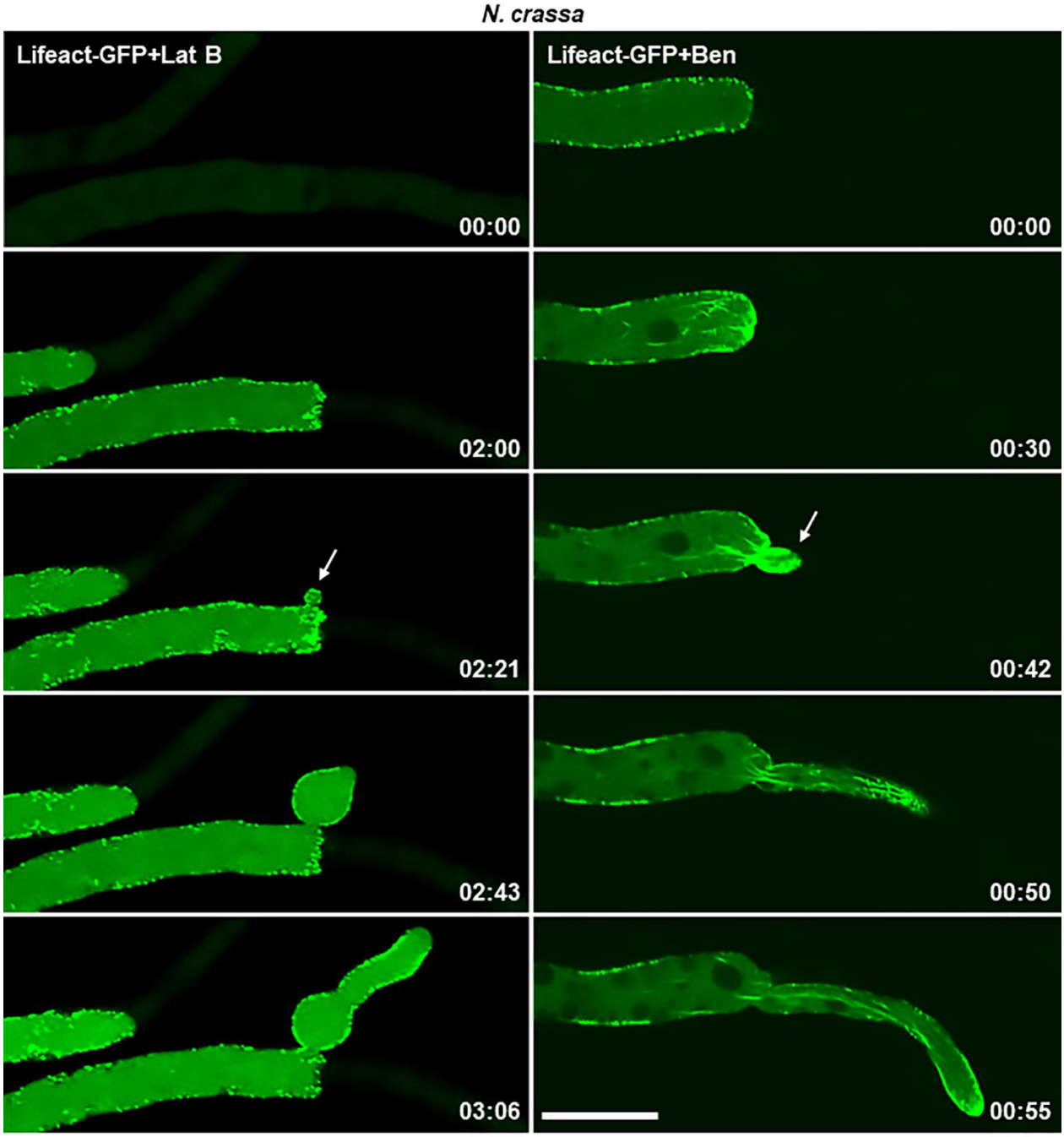

Figure 16. F-actin dynamics after mechanical injury in hyphae treated with actin inhibitor latrunculin B (Lat B) and microtubule inhibitor benomyl (Ben). Left panel is a time-lapse that shows F-actin dynamics in hyphae treated with Lat B (20 µg ml^{-1}). Hyphal regeneration is delayed in this condition, actin patches do not accumulate immediately after the scalpel cut and cables were not observed. Hyphae tend to develop lateral branches when they cannot emerge from the plugged septum (arrow; Time: 02:21). Right panel is a time-lapse that shows F-actin dynamics in hyphae treated with Ben (2.5 µg ml^{-1}). Hyphal regeneration is not affected even if microtubules are not polymerized. Arrow points at tip emergence (Time: 00:42). Scale bar = 20 µm. Time = hh:mm.

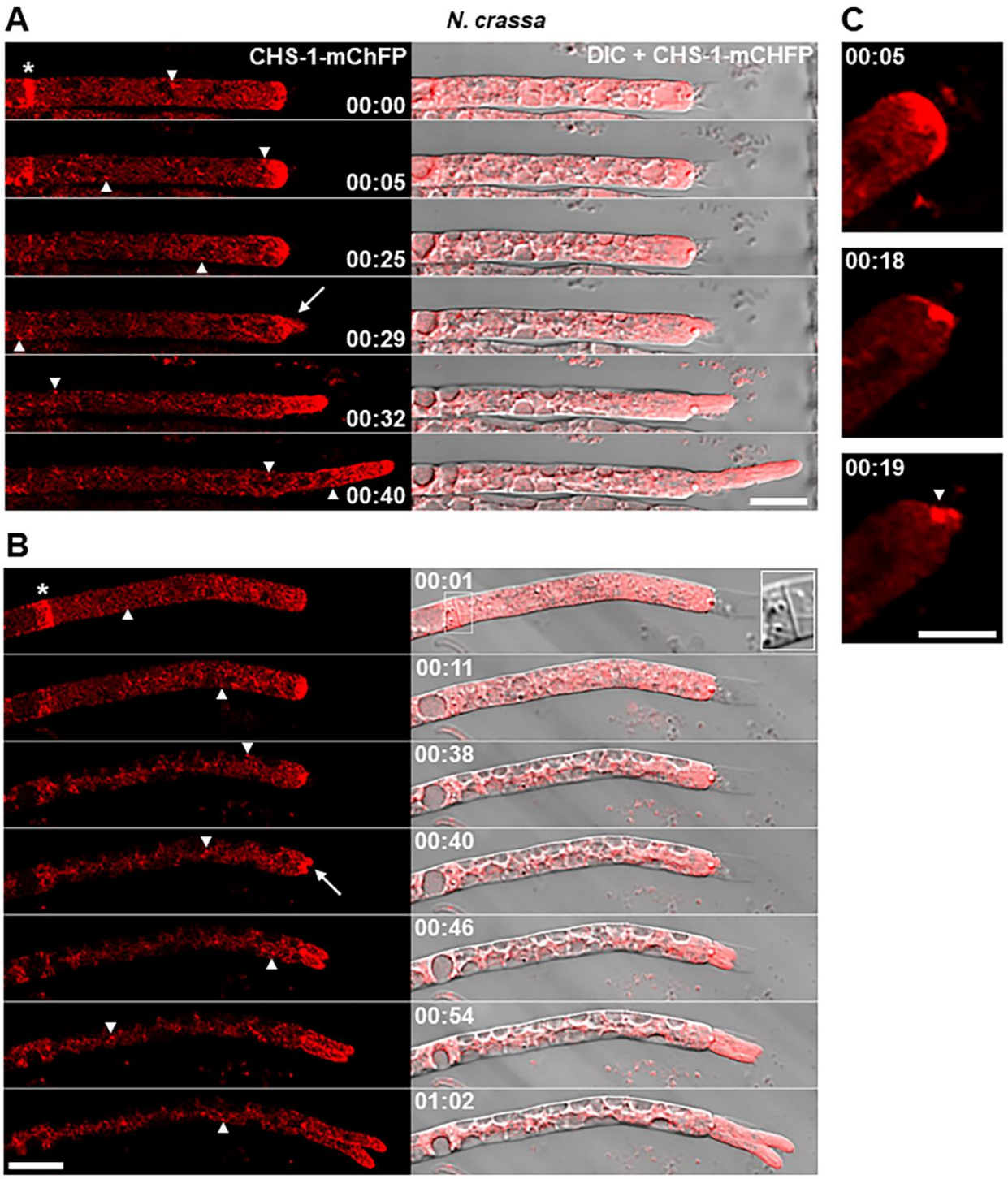

Figure 17. (A) Time-lapse shows chitin synthase 1 (CHS-1) tagged with mChFP after mechanical injury in *Neurospora crassa*. CHS-1 starts accumulating immediately at the plugged septum, forming a dome (Time: 00:05). Asterisk shows a developed septum, which fluorescence starts fading away after 5 minutes post-injury. Several bright puncta move throughout the hypha all the time (arrowheads). Arrow points to the accumulation of CHS-1 at the new emerging tip. Scale bar = 20 µm. (B) Time-lapse shows the CHS-1 dynamics during the regeneration of two new tips at one same hyphal compartment. Arrowheads point to scattered puncta throughout the hypha, asterisk to a developed septum with a zoom-in 1 min post-injury, and the arrow shows the emergence of the two tips. Scale bar = 20 µm. (C) Time-lapse shows CHS-1 distribution during regeneration after mechanical injury in *N. crassa*. ~16-18 min after the cut, CHS-1 signal narrows and concentrates at the Woronin body and the new emerging tip. Scale bar = 10 µm. Time = hh:mm.

3.4.2 Chitin synthase 1 localization in mechanically injured mycelium

We used the strain of *N. crassa* tagged with CHS-1-mCHFP to assess cell wall material deposition via exocytosis during the regeneration after injured hyphae (Figure 17). Immediately after the cut, CHS-1-mCHFP began accumulating at plugged septa, until a conspicuous dome was formed (~5 min after the cut). Additionally, CHS-1-mCHFP localized at developed septa adjacent to plugged septa, which eventually faded. Several dynamic bright puncta moved throughout the hypha. As the new hypha started forming, CHS-1-mCHFP was concentrated at site of tip emergence (Figure 17).

3.5 Determine the localization and dynamics of the early coat endocytic protein AP180

3.5.1 Localization and dynamics of AP180

N. crassa hyphae tagged with AP180-GFP were observed by laser-scanning confocal microscopy, as well as total internal reflection fluorescence microscopy (Figure 18) Conspicuous fluorescent patches of this protein were observed in the subapical collar (Figure 18A) (distance from the apex = 3.92 ± 0.62 µm, n=13, Figure 18). This structure kept a constant distance from the Spitzenkörper in growing hyphae. In the cases where hyphal extension stopped and the Spitzenkörper disassembled, the AP180-GFP patches reached the hyphal tip until growth resumed, and it returned to its typical subapical location. The width of the collar was 8.39 ± 0.9 µm (n=13). Patches in the collar are localized in the cell cortex as demonstrated by TIRFM in panel C, and LSCM in D of Figure 18, and they show both antero- and retrograde movement. Scattered patches were observed along the hyphae.

Additionally, during the formation of septa, AP180-GFP was transiently present (Figure 19). Scattered patches accumulated around the hyphal perimeter at the site of septum development. Later, AP180-GFP was observed as a single ring in the septum.

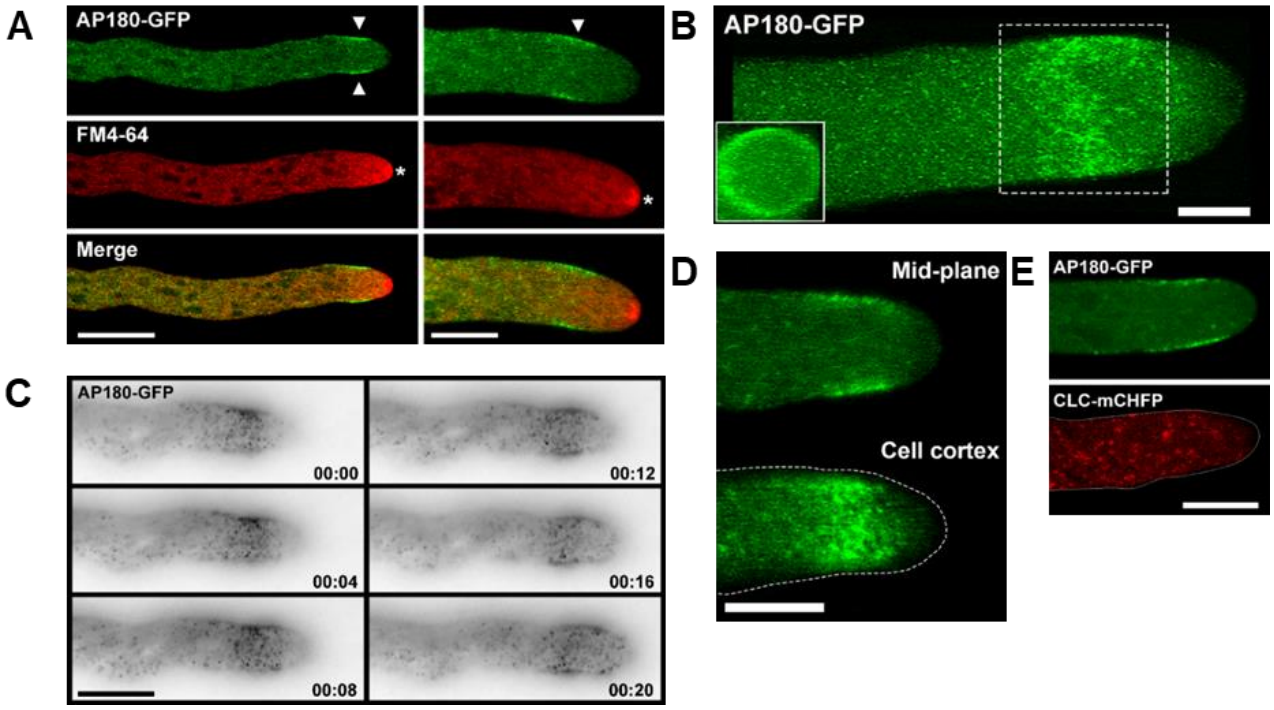

Figure 18. Localization of AP180-GFP in hyphae of *Neurospora crassa*. (A) This panel shows the localization of this protein, that being primarily in the subapex, coinciding with the endocytic collar (arrowheads); hyphae were stained with FM4-64 to show Spitzenkörper localization. Left scale bar = 10 µm, right scale bar = 5 µm. (B) 3D reconstruction of hyphal tip and a cross section that demonstrate AP180 forms a collar (bar = 5 µm). (C) TIRFM time-lapse shows the patches in the collar and some scattered patches; we observed that they can move in an anterograde and retrograde fashion. Scale bar = 10 µm. (D) Comparison between the mid-plane and the cell cortex of a hyphae tagged with AP180-GFP; here the concentration of patches in the cell cortex is visible, which is larger than that observed in the mid-plane. Scale bar = 10 µm). (E) Comparison between the localization of AP180-GFP and CLC-mCHFP in hyphal tips; interestingly AP180 is a part of the endocytic collar and clathrin is not. Scale bar = 10 µm. Time=hh:mm.

3.5.2 AP180 mutant characterization

We observed that the deletion of *ap180* was ascospore lethal. Ascospores of the Δ*ap180* strain did germinate, but they were not capable of establishing a colony. They grew bulky germ tubes that reached their maximum extension (~100 µm) 4 dpi before dying (Figure 20). The fact that the germ tubes looked bulky is due to periodic isotropic growth, ergo, loss of polarity. A homokaryotic Δ*ap180* strain was not possible to obtain, indicating that this gene is essential for *N. crassa*.

Next, we sought to determine if the deletion of the ANTH domain in AP180 was essential for cell viability, due to its importance in allowing this protein to bind to plasma membrane and accomplish its function as an endocytic adaptor.

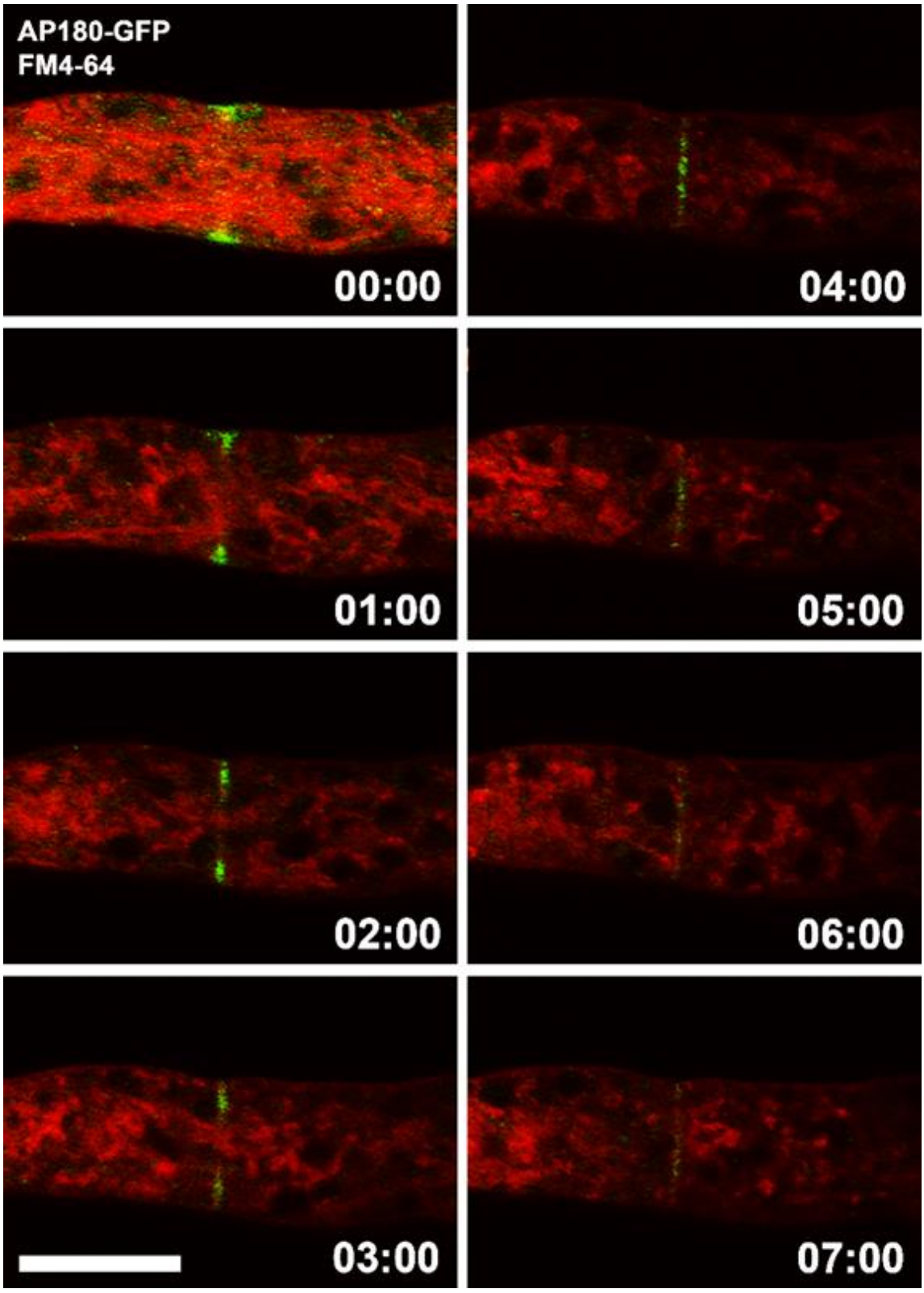

Figure 19. Localization of AP180-GFP during septum formation in *Neurospora crassa*. AP180-GFP patches begin to group in the periphery of the hypha, flanking the septation site. Then, they start forming a single-ring structure that corresponds to the septum. Scale bar = 10 µm. Time:mm:ss.

We constructed a mutant that lacks the ANTH domain (located in the N-terminus) and contains a GFP tag in its C-terminus, which allowed us to visualize its localization by confocal microscopy. Interestingly, we observed that AP180$^{\Delta ANTH}$-GFP was no longer aggregated forming a collar in the subapex but scattered in what seemed to be patches all throughout the hypha, including the apex (Figure 21). This strongly suggests that the ANTH domain was required for the localization of AP180 in the collar.

We also examined more distal areas in hyphae tagged with AP180Δ^{ANTH}-GFP and found that this protein does localize in septation sites during septa development (**¡Error! No se encuentra el origen de la referencia.**). Similar to the observation in the WT strain tagged with AP180-GFP, patches of the protein gathered at the periphery of the hypha flanking the septation site to form a single-ring (Figure 22A). We noticed numerous static patches in the periphery of the hyphae, in what seemed a nonspecific manner (Figure 22B). This was not observed in the AP180-GFP tagged strain.

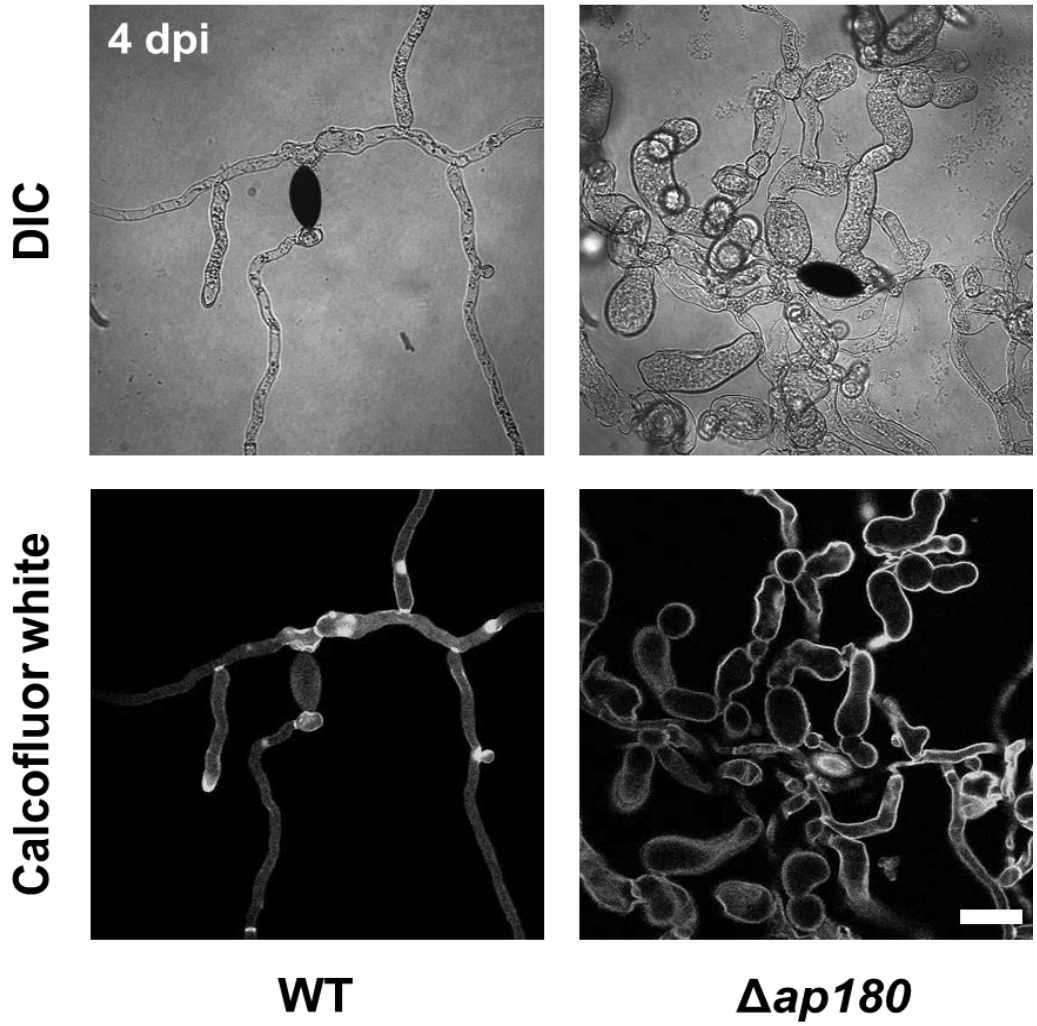

Figure 20. Phenotype of *Neurospora crassa* wild-type and Δ*ap180* ascospores 4 dpi. The deletion of *ap180* is ascospore lethal, which indicates that this protein in essential for cell viability. Δ*ap180* ascospores germinate but they are unable to establish a colony. Usually, their bulky germ tubes reach a length of ~100 µm before they die. Scale bar = 30 µm.

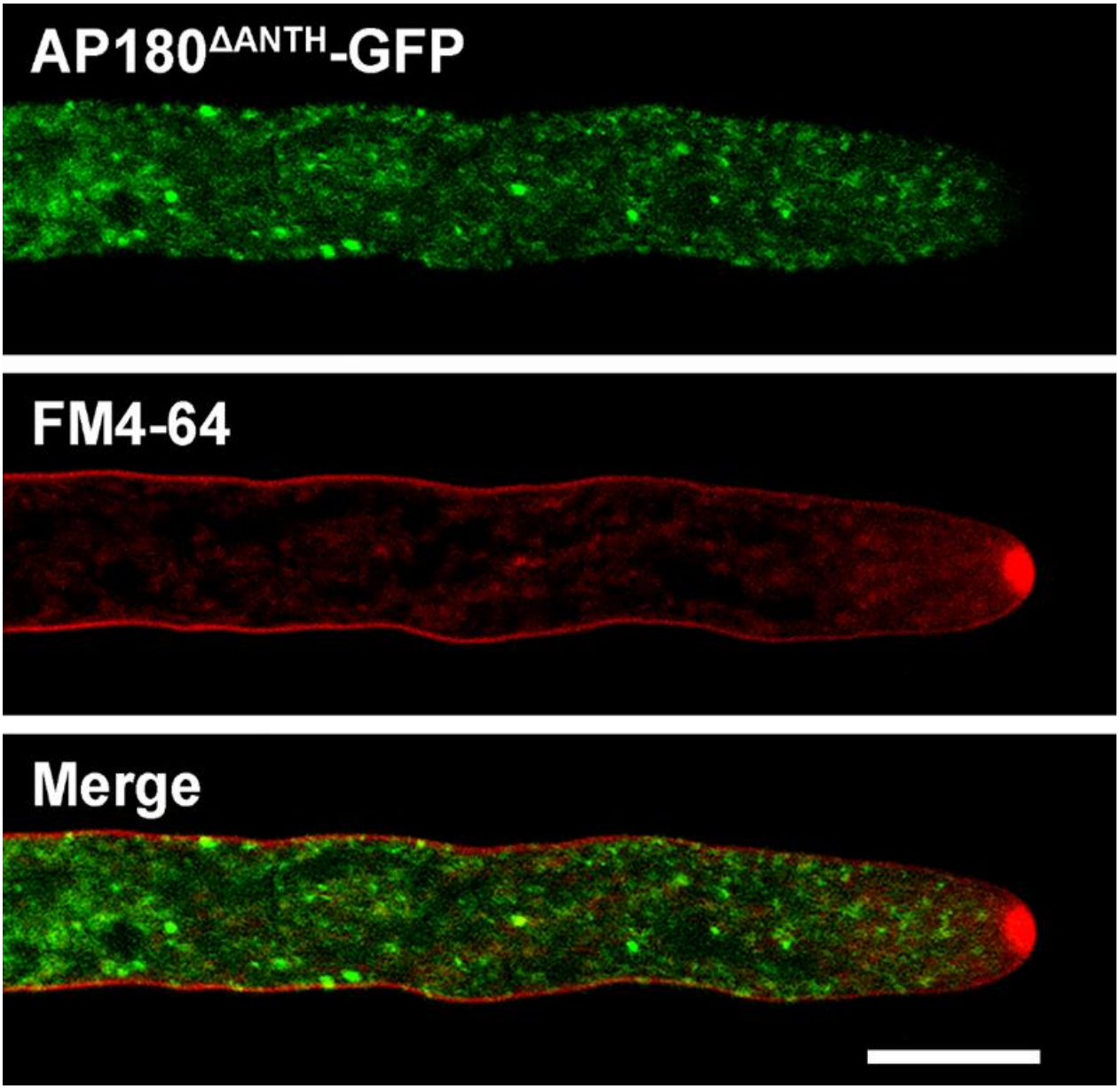

Figure 21. Localization of AP180Δ^{ANTH}-GFP in *Neurospora crassa*. AP180Δ^{ANTH}-GFP does not localize in the endocytic collar. Instead, the protein now shows as fluorescent spots throughout the hypha, suggesting that ANTH domain is required for the localization of this AP180 in the subapical collar. Scale bar = 10 µm.

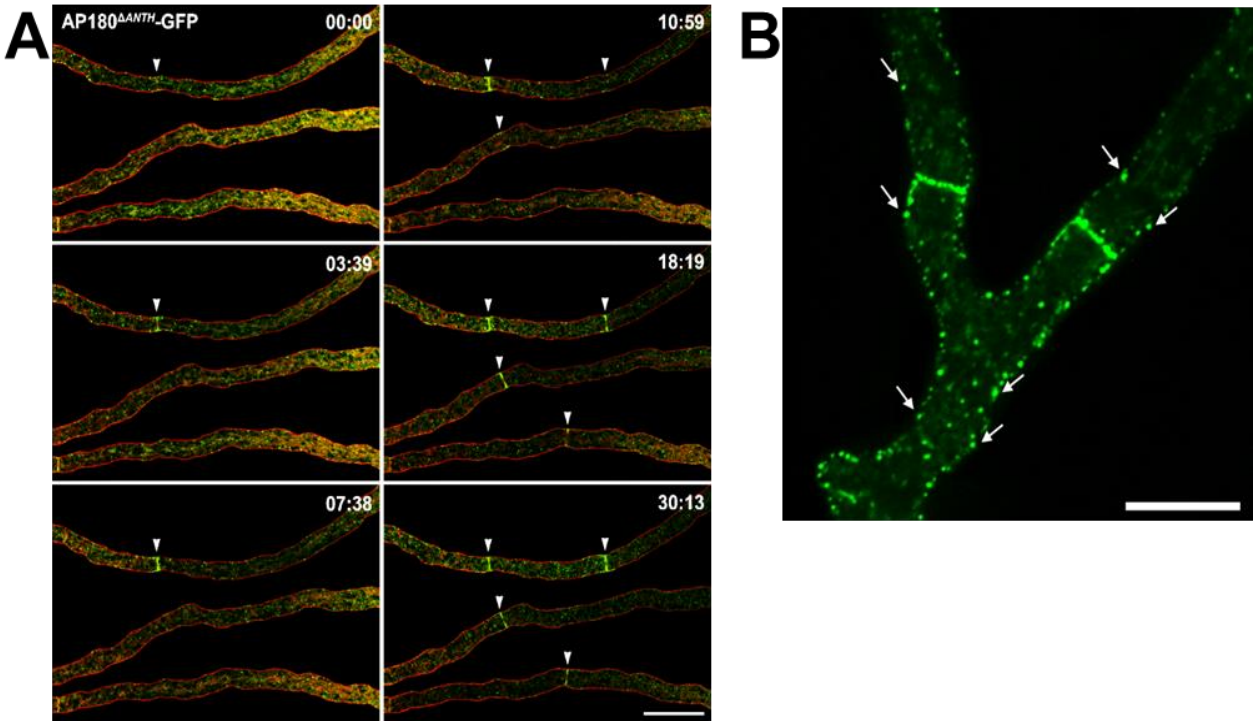

Figure 22. Localization of AP180$^{\Delta ANTH}$-GFP in more distal regions of hyphae in *Neurospora crassa*. (A) Time-lapse shows septation events in three different hyphae (arrowheads); protein forms single-rings in septation sites that apparently co-localize with the FM4-64 dyed membrane. Scale bar = 30 µm. Time=mm:ss. (B) Spinning-disk confocal image of two septation events; arrow indicate some of the static patches observed in the periphery of the hyphae. Scale bar = 10 µm.

3.5.3 AP180-GFP immunoprecipitation

To look for possible interactor of AP180, we performed IP-MS/MS of AP180-GFP. First, we verified the presence of AP180 by Western blot (Figure 23). Next, we identified 158 proteins as possible interactors (see Annexes). In our ranking, the protein with the highest value was an uncharacterized protein (NCU08889). It probably has zinc metallopeptidase activity due to its zinc-binding site (active site), also, it may be involved in signal transduction because it has serine/threonine protein kinase activity. This has orthologs in other fungal species. In *N. discreta*, the ortholog has been annotated as a chitinase. However, in all the other organism where it can be found it has been annotated as a putative and/or uncharacterized protein as well.

An interesting possible interactor is profilin (NCU06397), which is a small protein that binds to actin and affects the structure of the cytoskeleton. At high concentrations, profilin prevents the polymerization of actin, whereas it enhances it at low concentrations. In addition, we found an actin cross-linking protein

(NCU10360) annotated as an uncharacterized protein. This protein contains two Kelch domains and proteins containing these domains act as substrate adaptor for Cullin 3 ubiquitin ligases.

Additionally, we found the amphiphysin-like lipid raft protein *amph*-1 (NCU01069), an ortholog of Rvs161p and Rvs167p in *S. cerevisiae* and Hob3 in *Schizosaccharomyces pombe*. Amphiphysins are interesting proteins because they have an actin cortical patch localization and are involved in endocytosis, also, they contain BAR domains (inducer of membrane tubulation). Amphiphysins act in the cleavage step of CME.

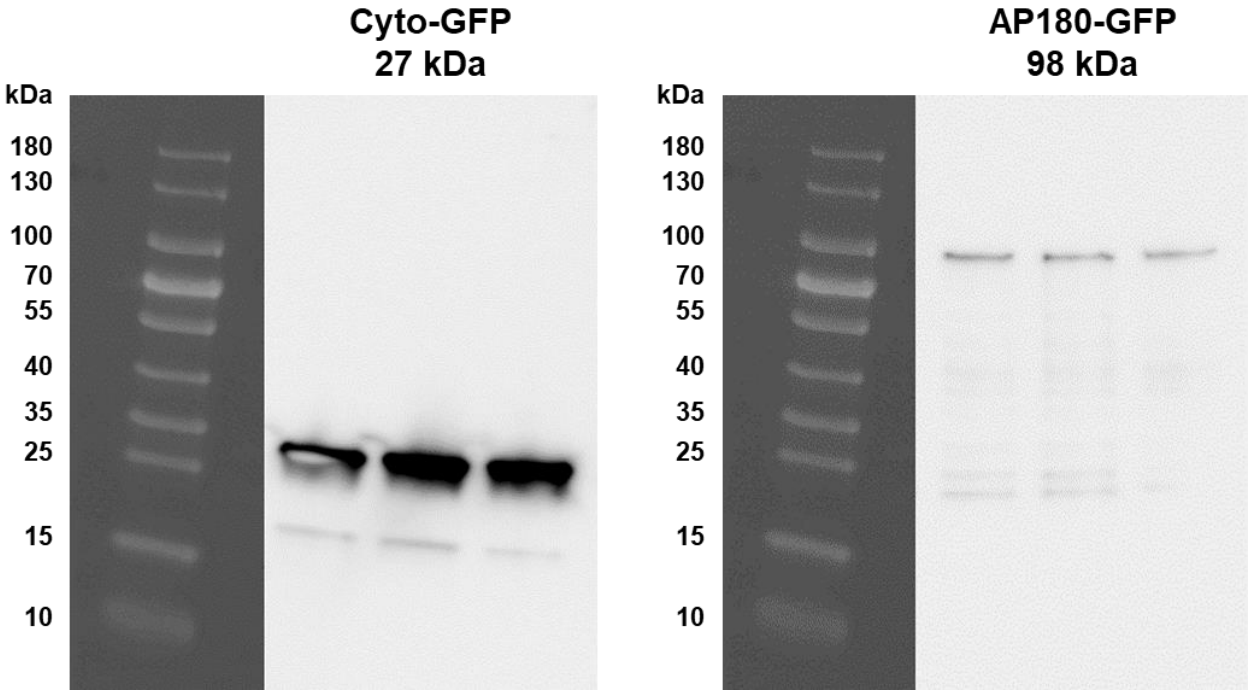

Figure 23. Western blot showing the presence of Cyto-GFP (27 kDa) and AP180-GFP (98 kDa). Experiments were carried out by triplicate, as shown in the figure.

Chapter 4. Discussion

4.1 Experimental measurement of endocytosis in mature hyphae

As we reported in Bartnicki-García et al. (2018), we believe this is the first successful attempt to quantitate the endocytic process in fungi. Given uncertainties as to the actual size of an endocytic vesicle, the exact boundaries of the endocytic collar dimension, and the accuracy of the photobleaching procedure, the calculated value for endocytosed membrane, namely 12.5%, should be considered as a first approximation of the exocytosis/endocytosis ratio. In the absence of measurements of the endocytic vesicles of *N. crassa*, we relied on images of "filasomes" (~10 nm) of *Sclerotium rolfsii* (Roberson, 1992). Filasomes are likely to be bona fide endocytic vesicles, as evidenced by their microvesicular size, their peripheral localization in the cell, and the network of actin filaments surrounding them (Roberson, 1992; Takagi, 2003). Accurate vesicle size is essential to obtain realistic measurement of membrane dynamics not only for endocytic but also exocytic vesicles. Thus, the more reliable measurements of exocytic vesicles obtained by cryofixation of *N. crassa* (Roberson et al., 2010) namely 0.08 μm in diameter are substantially smaller than the 0.10 μm values for chemically fixed hyphae used by Collinge and Trinci (1974). Accordingly, we have revised upward the frequently cited figure for vesicle discharge in a hypha of *N. crassa* growing at full speed from 38,000 to 59,000 vesicles per min (Collinge and Trinci, 1974), and this itself may be an underestimate that does not include the additional number of vesicles calculated from the amount of membrane internalized by endocytosis.

The finding that exocytosis generates an excess of plasma membrane supports our conclusion that the primary role of endocytosis is to dispose of this membrane excess. The positioning of the endocytic collar a few micrometers behind the apex creates an efficient tandem operation between membrane insertion at the apex of a hypha and membrane internalization in the subapex; the possibility that some physical coordination may exist between these processes could be a fruitful topic future investigation. Besides membrane recycling, the endocytic process is being actively investigated by other researches as a mechanism for recycling proteins of importance in apical growth (Commer et al., 2020; Hernández-González et al., 2018; Higuchi et al., 2009; Peñalva, 2010; Schultzhaus and Shaw, 2015; Steinberg, 2007).

The internalization of membrane during endocytosis must be an energy demanding process needed to force the membrane against the high turgor pressure of the fungal cytosol. We can speculate that such expensive process evolved to support the intense exocytosis that allows fungal hyphae to exert their

superior qualities, rapid colonization of the environment by fast growth rate and effective substrate utilization by abundant secretion of substrate degrading enzymes. Endocytosis became an efficient solution to recycle the excess of membrane generated by exocytosis.

4.2 Endocytosis and nutrients stress

Strikingly, we found that there are far more endocytic events occurring in hyphae grown in water agarose (VMM 0%), where there is less growth, than in hyphae grown in VMM 100%. This finding contradicts our hypothesis that states: “the endocytic rate is lower when there is a decrease of hyphal growth.” A possible explanation of this is that exocytic vesicles, which cause the membrane excess, might not be only transporting cell wall synthesis enzymes and material, but also hydrolytic enzymes to degrade the medium and obtain the most of it to nurture. It would be necessary to screen what molecules is the fungus excreting into both media and if there is a real difference between the two conditions.

In our FM4-64 internalization experiments we observed that in both VMM and WA, the fluorescence intensity increase through time was the same. Although we would expect a faster internalization in the WA condition in agreement with our FRAP experiments, we have certainty of one thing, and that is that less growth does not translate in less endocytosis. Therefore, we strongly believe that even in poor growth conditions endocytosis is playing a key role in maintaining the hyphal shape, not only by membrane remodeling, but also by removing polarity factors and transporters embedded in the plasma membrane (Shaw et al., 2011).

We are yet to assess why our FRAP and FM4-64 internalization results do not completely correspond each other, however, sets of data might suggest that exocytosis is not only involved in cell wall synthesis and membrane extension, and endocytosis a process that only responds to it. We might need to re-think the way we have been addressing exocytosis and endocytosis in fungal cell biology in the past. Without a question, a lot remains to be revealed regarding these closely related cellular processes.

4.3 Genesis of the endocytic collar

We followed the localization and dynamics of endocytic patches tagged with either FIM-1-GFP or FIM-1-mCHFP, from unswollen (ungerminated) conidia to long germlings. In agreement with a previous study from our group (Lara-Rojas et al., 2016), we observed that in conidia, endocytic patches are scattered throughout the cell cortex and increase through time. Once the germ tube emerges, besides being scattered, the endocytic patches start accumulating conspicuously at the very tip forming a cap that will later take its predominant subapical position as a collar. We strongly believe that growth rate (v≥0.5 µm min^{-1}) is associated with the position of the endocytic collar, as exocytosis is what keeps the collar in the subapex. The moment exocytosis becomes larger and the Spitzenkörper is noticeable (due to exocytic vesicles accumulation), there is no space for the endocytic patches to remain at the apex, therefore, they are restricted to the subapical region. The use of a better exocytosis marker than CHS-1-GFP is necessary to further demonstrate this, as the signal of this is weak and it is easily eclipsed by fimbrin signal due to its high abundance in the cell. By doing so, we are confident that we will be able to capture the whole picture of the endocytic collar and Spitzenkörper relation.

We propose a new model to depict the establishment of the endocytic collar called “From cap to collar” (Figure 24).

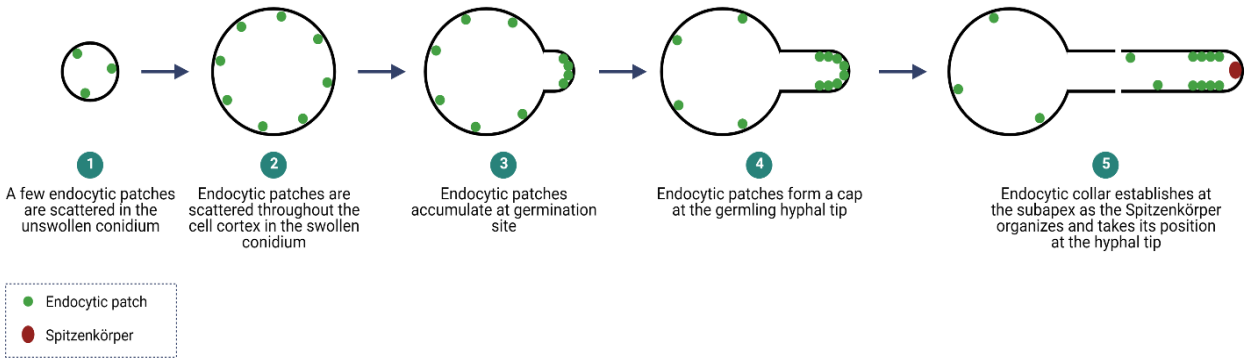

Figure 24. Model “From cap to collar”. Model depicts the distribution and accumulation of actin patches through time during germination and germling growth. Initially, a few patches are scattered throughout the conidium, and once the conidium swollen the patches become more numerous. Patches start accumulating in the site of tip emergence and as the tube elongates patches arrange in a “cap”-like structure. When exocytosis becomes higher and the young hypha reaches a v≥0.5 µm min^{-1}, there is a switch from cap (apex) to collar (subapex).

4.4 Actin endocytic patches role in hyphal regeneration

In *N. crassa*, as in other filamentous fungi, actin is found in different forms: at filaments in the core of the Spitzenkörper, as patches at the endocytic collar, as actomyosin tangles and contractile rings at septation sites, and as patches and cables along the hypha. Our results indicate an active role of actin in hyphal growth recovery and re-establishment of polarity.

As we reported in Garduño-Rosales et al. (2022), our observations by confocal microscopy coincided with earlier findings by Trinci and Collinge (1974) who described the occlusion of septal pores of damaged hyphae of *N. crassa* by hexagonal crystals (hexagonal Woronin bodies). They observed that the hexagonal crystals appeared to be membrane bound and associated to mature septa in untreated hyphae. After damage, substantial loss of cytoplasm and organelles from more distal compartments was prevented by the occlusion of septal pores by the hexagonal crystals (Supplementary Figure 1A). These crystals were often covered on one side with electron transparent material (cell wall) which was continuous with the septal wall. Vesicles were observed to accumulate behind the plugged septa. We found that after mechanical injury, hyphae regenerated by growing new intrahyphal hyphae, matching the findings of Trinci and Collinge (1974).

Actin might play a major role accumulating at the region where a new hypha will grow, probably to re-organize the tip growth apparatus. We mainly observed actin patches accumulated in this region, which are known to be sites of endocytosis (Goode et al., 2015). We followed the dynamics of CHS-1 (Sánchez-León et al., 2011), an exocytic marker, during hyphal regeneration, and found that it accumulated in a conspicuous manner at plugged septa. Endocytosis and exocytosis are coupled processes, as endocytosis is an efficient solution to recycle the excess of membrane generated by exocytosis (Bartnicki-Garcia et al., 2018). Therefore, we hint that in addition to the involvement of F-actin in exocytosis, actin patches at the plugged septum are probably remodeling the plasma membrane via endocytosis as a response to the excess generated by the incorporation of exocytic vesicles, just as it occurs at the endocytic collar behind the apex (Bartnicki-Garcia et al., 2018). We normally observed the re-organization of the Spitzenkörper and the endocytic collar within 1 h post-mechanical injury. Interestingly, actin dynamics during hyphal regeneration are highly similar to the establishment of the endocytic collar in germlings, especially the accumulation of endocytic actin patches at site of hyphal emergence, forming a conspicuous cap once the tip emerges and then differentiates into the endocytic collar at hyphal subapex.

The fact that hyphal regeneration was severely altered and delayed when adding actin inhibitor Lat B further supports the importance of the F-actin role in this process. Benomyl did not affect hyphal regeneration which suggests that microtubules are not necessary to attain it.

In animal cells, the Yes-Associated Protein 1 (Yap1) is a key component of the Hippo signaling pathway, which regulates cell proliferation and apoptosis (Huang et al., 2005; Miesfeld and Link, 2014; Sudol et al., 1995). Yap directly regulates genes encoding cell cycle progression proteins and genes encoding proteins that promote F-actin polymerization and that link the actin cytoskeleton to the extracellular matrix (Morikawa et al., 2015). It has been observed that actin high order structures support plasma membrane recovery in various organisms, for example, the actomyosin purse string in Xenopus oocytes (Bement et al., 1999). However, although plasma membrane repair is of central concern in cell repair in animal cells, amoebae, and yeast, after injury (Bi et al., 1995; Kono et al., 2012; Szubinska, 1971; Togo et al., 1999), in septate fungi cell recovery is a matter related mainly to cell wall rather than membrane repair, after the septal pore is plugged by Woronin bodies.

An important finding of our studies was the involvement of septa play in the regeneration of the injured hyphae. Besides their key role in stopping a catastrophic loss of cytoplasmic content, new septation events in close proximity to plugged septa seem to be crucial for hyphal regeneration. For septation to occur in fungal cells, F-actin and associated proteins participation is essential; in injured hyphae as in normal ones, the first evidence of septum development is the assembly of a broad tangle of long actomyosin cables, the SAT, which constricts to form a tight ring, the CAR (Delgado-Álvarez et al., 2014).

We identified double septa plugging, specifically the two septa adjacent to the injury site, which is not a common phenomenon in reports using scalpels and/or razor blades to cut the mycelia, but it is often observed in hyphae damaged by water flooding (Trinci and Collinge, 1974). Double septa plugging may or not may occur depending on the extension of the damage, probably to further support hyphal survival. In our observations of this event, the new tip emerged from the second plugged septum farther from the injury site. Interestingly, once the tip reached the first plug it was unable to surpass it even after one hour. The second plug is an obstacle that cannot be penetrated by the new hyphal tip. A gradual remodeling occurring in the septal cell wall into an apical cell wall takes place. We speculate that in addition to wall synthesis there must be lytic enzymes acting simultaneously, conferring plasticity to the cell wall to withstand internal turgor pressure, as previously proposed by Bartnicki-Garcia (1973) in growing hyphal tips.

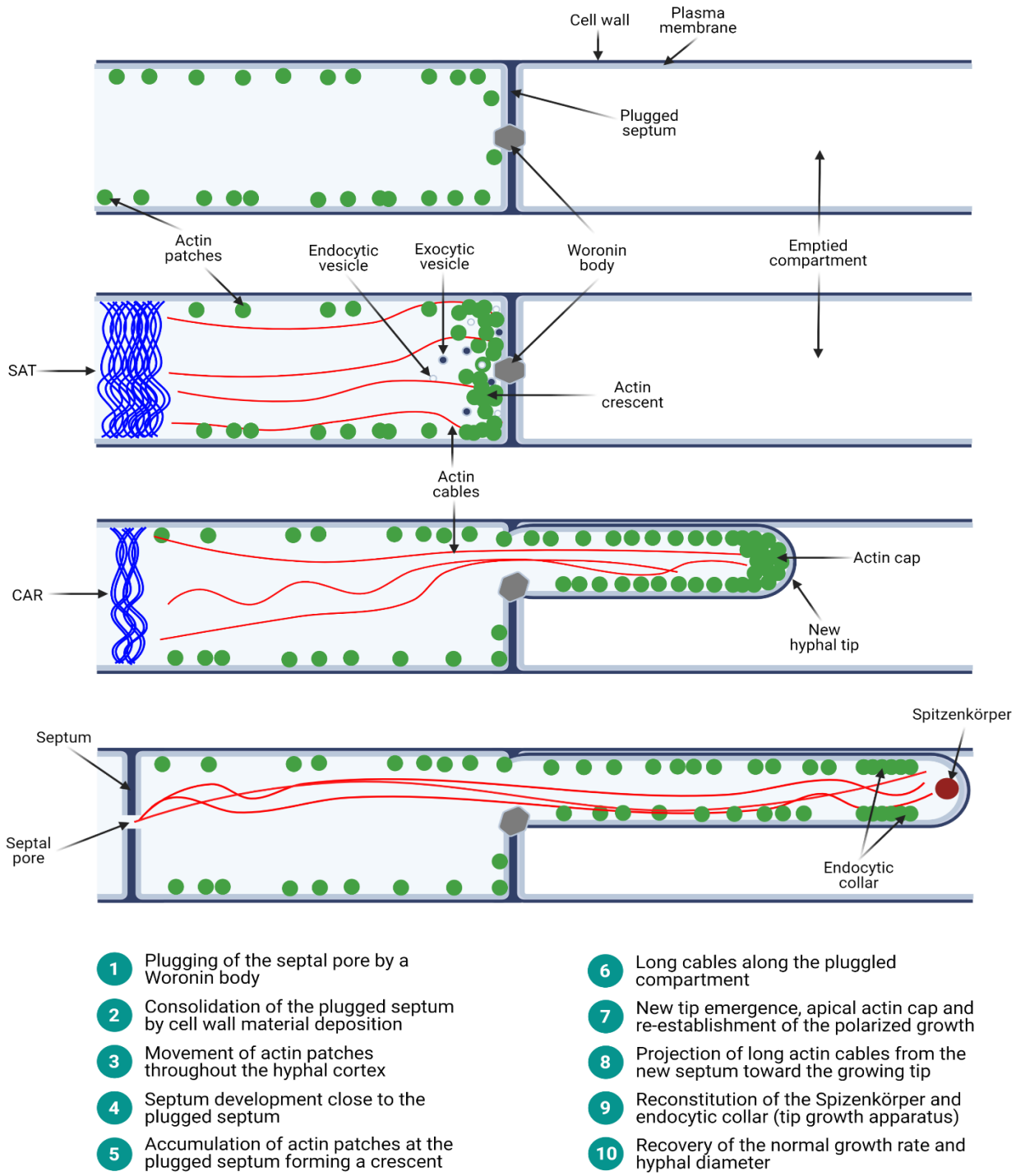

Figure 25. Model of polarized growth recovery in an injured hypha. The septum closest to the injury site becomes plugged by a Woronin body, followed by sealing of the plug with cell wall material during the consolidation phase, preventing further cytoplasm bleeding. The deposition of cell wall material must be carried through exocytic vesicles. Actin patches outlining the periphery of the plugged hyphal compartment move fast along the cell, in both anterograde and retrograde fashion. A septal actomyosin tangle starts developing near the plugged septum, and then it coalesces into a contractile actomyosin ring to form a new septum. Actin patches progressively accumulate at the plugged septum and actin cables are visible, probably transporting vesicles. The actin patches at the septum organize into an actin crescent, from which the new tip emerges re-establishing the polarized growth, moving the plug to the side. The actin crescent becomes an actin cap. Long actin cables project from the new septum toward the growing tip. The actin cap differentiates to reconstitute the hyphal tip growth apparatus (Spitzenkörper and endocytic collar). Eventually, the new hypha recovers its normal growth rate and diameter.

This does not occur at the first plugged septum, therefore, the regenerated hypha cannot pass, which suggests that due to the lack of wall remodeling in that plug the hypha hits an obstacle that leaves it trapped.

Our observations are summarized in Figure 25, which shows how F-actin starts reorganizing immediately after mechanical injury in *N. crassa*. Actin patches accumulate in the hyphal compartment adjacent to the plugged compartment. The finding that new septa develop before growth resumes suggests that this process is essential for hyphal regeneration, hence, survival. The actin dynamics we observed in regenerating hyphae is essentially the recovery of a normal physiology process to resume apical growth. Actin cytoskeleton is indispensable to re-establish the tip growth apparatus, hence, apical polarized growth. Similar findings on F-actin and CHS-1 dynamics led us to conclude that the actin cytoskeleton plays a key role in hyphal regeneration due to its function as the conveyor of the vesicles responsible for new cell wall growth and supporting membrane remodeling via endocytosis, re-shaping the plugged septum into the new apical dome.

4.5 Early phase of endocytosis

To explore the early phase of endocytosis we visualized the early arriving endocytic coat protein AP180, which has been traditional considered a clathrin adaptor (Morris et al., 1993). However, our data and studies in *A. nidulans* (Schultzhaus et al., 2017) indicate that clathrin is not part of the endocytic collar. Our microscopy experiments support that AP180 is an endocytic protein, part of the endocytic patches in the collar. Something that would be interesting to do is co-express AP180-GFP with a late endocytic reporter, e.g. fimbrin, to locate it in time of endocytic patch life span.

The phenotype of the Δ*ap180* mutant shows that the lack of AP180 is lethal, as ascospores grow bulky non-functional hyphae that are unable to establish a colony. Deletion of genes that encode endocytic proteins often results in aberrant hyphal morphology, however, they survive (Echauri-Espinosa et al., 2012; Lara-Rojas et al., 2016), which indicates redundance in endocytic proteins functions. Interestingly, AP180 is essential, and this arise the question if this is because it is necessary to establish the endocytic site. In yeast, it is known that Ede1 is the first protein to arrive to the endocytic site and that it interacts with other downstream endocytic proteins, influencing their life span (Boeke et al., 2014; Lu and Drubin,

2017). One of these proteins is in fact the yeast homolog of AP180, Yap1801/2. Could it be that AP180 is indispensable for endocytosis in *N. crassa*? That is a lead worth pursuing.

The ANTH domain allows AP180 to bind to membrane lipids (Ford et al., 2001). The mutant of AP180 lacking the N-terminal ANTH domain (AP180Δ^{ANTH}-GFP) is not forming a collar, but still manages to have a normal morphology and growth rate. This finding suggests that the ANTH domain although necessary for organizing AP180 containing patches in a collar, is not essential for the functionality of the protein, hence, survival of the microorganism. Probably, the most important part of the structure of AP180 is in the rest of the protein, which is known to contain DxF motifs that allow it to interact with other endocytic proteins (Ford et al., 2001). Probably, the most important role of AP180 is the interaction it has with downstream proteins.

In our IP-MS/MS data we found that AP180 may interact with actin-binding proteins, actin cross-linkers and amphiphysins. This is interesting because these proteins act in the late stages of endocytosis, indicating the importance of AP180 in the recruitment of downstream endocytic proteins. However, the protein with highest value was an uncharacterized protein codified by the gene NCU08889. Studying this novel protein may be interesting and helpful to further assess the role of AP180. Additionally, we did not find clathrin as a possible interactor, which supports the notion that clathrin does not regulate endocytosis in the subapical collar of *N. crassa*.

Chapter 5. Conclusions

- Exocytosis generated an excess of plasma membrane. About 12.5% of the exocytosed membrane was recycled by endocytosis.

- There seemed to be more endocytic events in hyphae grown in scarcity of nutrients than in standard conditions. Nevertheless, rate of FM4-64 internalization was the same in hyphae grown in scarcity of nutrients and in standard conditions.

- The establishment of the subapical endocytic collar started with endocytic patches organized as a cap at the very tip of the germ tube. The cap switched into a collar when the hyphal elongation rate reached ≥0.5 μm min^{-1}.

- AP180 is an essential protein of the early coat of endocytic vesicles. AP180 localization is ANTH domain-depended. AP180 was not associated with clathrin.

- Cell wall and plasma membrane needed to be remodeled to re-establish polarized growth in mechanically injured hyphae. Unlike microtubules, actin was essential for hyphal regeneration and re-establishment of polarized growth following mechanical injury. Septa development was necessary for hyphal regeneration following mechanical injury.

Cited literature

Adams, A.E., Botstein, D., and Drubin, D.G. 1991. Requirement of yeast fimbrin for actin organization and morphogenesis *in vivo*. Nature *354*, 404-408.

Ahle, S., and Ungewickell, E. 1986. Purification and properties of a new clathrin assembly protein. The EMBO Journal *5*, 3143-3149.

Arai, R., Nakano, K., and Mabuchi, I. 1998. Subcellular localization and possible function of actin, tropomyosin and actin-related protein 3 (Arp3) in the fission yeast *Schizosaccharomyces pombe*. European Journal of Cell Biology *76*, 288-295.

Araujo-Bazán, L., Peñalva, M.A., and Espeso, E.A. 2008. Preferential localization of the endocytic internalization machinery to hyphal tips underlies polarization of the actin cytoskeleton in *Aspergillus nidulans*. Molecular Microbiology *67*, 891-905.

Atkinson, H.A., Daniels, A., and Read, N.D. 2002. Live-cell imaging of endocytosis during conidial germination in the rice blast fungus, *Magnaporthe grisea*. Fungal Genetics and Biology *37*, 233-244.

Ayscough, K.R., Stryker, J., Pokala, N., Sanders, M., Crews, P., and Drubin, D.G. 1997. High rates of actin filament turnover in budding yeast and roles for actin in establishment and maintenance of cell polarity revealed using the actin inhibitor latrunculin-A. The Journal of Cell Biology *137*, 399-416.

Bartnicki-Garcia, S. 1973. Fundamental aspects of hyphal morphogenesis. Paper presented at: Microbe Differentiation 23rd Symposium of the Society of General Microbiology (Cambridge University Press).

Bartnicki-García, S. 2002. Hyphal tip growth. In Molecular Biology of Fungal Development, H.D. Osiewacz, ed. (Marcel-Dekker, Inc.), pp. 22-58.

Bartnicki-García, S., Garduño-Rosales, M., Delgado-Álvarez, D.L., and Mouriño-Pérez, R.R. 2018. Experimental measurement of endocytosis in fungal hyphae. Fungal Genetics and Biology *118*, 32-36.

Bement, W.M., Mandato, C.A., and Kirsch, M.N. 1999. Wound-induced assembly and closure of an actomyosin purse string in *Xenopus* oocytes. Current Biology : CB *9*, 579-587.

Berepiki, A., Lichius, A., Shoji, J.Y., Tilsner, J., and Read, N.D. 2010. F-actin dynamics in *Neurospora crassa*. Eukaryotic Cell *9*, 547-557.

Bi, G.Q., Alderton, J.M., and Steinhardt, R.A. 1995. Calcium-regulated exocytosis is required for cell membrane resealing. The Journal of Cell Biology *131*, 1747-1758.

Boeke, D., Trautmann, S., Meurer, M., Wachsmuth, M., Godlee, C., Knop, M., and Kaksonen, M. 2014. Quantification of cytosolic interactions identifies Ede1 oligomers as key organizers of endocytosis. Molecular Systems Biology *10*, 756.

Bozkurt, T.O., Schornack, S., Win, J., Shindo, T., Ilyas, M., Oliva, R., Cano, L.M., Jones, A.M., Huitema, E., van der Hoorn, R.A*., et al.* 2011. *Phytophthora infestans* effector AVRblb2 prevents secretion of a plant immune protease at the haustorial interface. Proceedings of the National Academy of Sciences of the United States of America *108*, 20832-20837.

Brach, T., Godlee, C., Moeller-Hansen, I., Boeke, D., and Kaksonen, M. 2014. The initiation of clathrin-mediated endocytosis is mechanistically highly flexible. Current Biology *24*, 548-554.

Bretscher, A. 2003. Polarized growth and organelle segregation in yeast: the tracks, motors, and receptors. The Journal of Cell Biology *160*, 811-816.

Brodsky, F.M. 1988. Living with clathrin: its role in intracellular membrane traffic. Science *242*, 1396-1402.

Brodsky, F.M., Chen, C.Y., Knuehl, C., Towler, M.C., and Wakeham, D.E. 2001. Biological basket weaving: formation and function of clathrin-coated vesicles. Annual Review of Cell and Developmental Biology *17*, 517-568.

Chvatchko, Y., Howald, I., and Riezman, H. 1986. Two yeast mutants defective in endocytosis are defective in pheromone response. Cell *46*, 355-364.

Cole, L., Orlovich, D.A., and Ashford, A.E. 1998. Structure, function, and motility of vacuoles in filamentous fungi. Fungal Genetics and Biology *24*, 86-100.

Collinge, A.J., and Trinci, A.P.J. 1974. Hyphal tips of wild-type and spreading colonial mutants of *Neurospora crassa*. Archives of Microbiology *99*, 353-368.

Commer, B., Schultzhaus, Z., and Shaw, B.D. 2020. Localization of NPFxD motif-containing proteins in *Aspergillus nidulans*. Fungal Genetics and Biology *141*, 103412.

Davis, R.H. 2000. *Neurospora*: Contributions of a Model Organism (OUP USA).

Delgado-Álvarez, D.L., Bartnicki-García, S., Seiler, S., and Mouriño-Pérez, R.R. 2014. Septum development in *Neurospora crassa*: the septal actomyosin tangle. PloS One *9*, e96744.

Delgado-Álvarez, D.L., Callejas-Negrete, O.A., Gomez, N., Freitag, M., Roberson, R.W., Smith, L.G., and Mouriño-Pérez, R.R. 2010. Visualization of F-actin localization and dynamics with live cell markers in *Neurospora crassa*. Fungal Genetics and Biology *47*, 573-586.

Doyle, T., and Botstein, D. 1996. Movement of yeast cortical actin cytoskeleton visualized *in vivo*. Proceedings of the National Academy of Sciences of the United States of America *93*, 3886-3891.

Dulic, V., and Riezman, H. 1989. Characterization of the END1 gene required for vacuole biogenesis and gluconeogenic growth of budding yeast. The EMBO Journal *8*, 1349-1359.

Echauri-Espinosa, R.O., Callejas-Negrete, O.A., Roberson, R.W., Bartnicki-García, S., and Mouriño-Pérez, R.R. 2012. Coronin is a component of the endocytic collar of hyphae of *Neurospora crassa* and is necessary for normal growth and morphogenesis. PloS One *7*, e38237.

Engqvist-Goldstein, A.E., and Drubin, D.G. 2003. Actin assembly and endocytosis: from yeast to mammals. Annual Review of Cell and Developmental Biology *19*, 287-332.

Ford, M.G., Pearse, B.M., Higgins, M.K., Vallis, Y., Owen, D.J., Gibson, A., Hopkins, C.R., Evans, P.R., and McMahon, H.T. 2001. Simultaneous binding of PtdIns(4,5)P2 and clathrin by AP180 in the nucleation of clathrin lattices on membranes. Science *291*, 1051-1055.

Fuchs, U., Hause, G., Schuchardt, I., and Steinberg, G. 2006. Endocytosis is essential for pathogenic development in the corn smut fungus *Ustilago maydis*. The Plant Cell *18*, 2066-2081.

Garduño-Rosales, M., Callejas-Negrete, O.A., Medina-Castellanos, E., Bartnicki-García, S., Herrera-Estrella, A., and Mouriño-Pérez, R.R. 2022. F-actin dynamics following mechanical injury of *Trichoderma atroviride* and *Neurospora crassa* hyphae. Fungal Genetics and Biology *159*, 103672.

Gierz, G., and Bartnicki-Garcia, S. 2001. A three-dimensional model of fungal morphogenesis based on the Vesicle Supply Center concept. Journal of Theoretical Biology *208*, 151-164.

Girbardt, M. 1969. Die Ultrastruktur der Apikalregion von Pilzhyphen. Protoplasma *67*, 413-441.

Goode, B.L., Eskin, J.A., and Wendland, B. 2015. Actin and endocytosis in budding yeast. Genetics *199*, 315-358.

Grove, S.N., and Bracker, C.E. 1970. Protoplasmic organization of hyphal tips among fungi: vesicles and Spitzenkörper. Journal of bacteriology *104*, 989-1009.

Harris, S.D., Read, N.D., Roberson, R.W., Shaw, B., Seiler, S., Plamann, M., and Momany, M. 2005. Polarisome meets Spitzenkörper: microscopy, genetics, and genomics converge. Eukaryotic Cell *4*, 225-229.

Hernández-González, M., Bravo-Plaza, I., Pinar, M., de Los Rios, V., Arst, H.N., Jr., and Peñalva, M.A. 2018. Endocytic recycling via the TGN underlies the polarized hyphal mode of life. PLoS Genetics *14*, e1007291.

Hickey, P.C., Jacobson, D., Read, N.D., and Glass, N.L. 2002. Live-cell imaging of vegetative hyphal fusion in *Neurospora crassa*. Fungal Genetics and Biology *37*, 109-119.

Higuchi, Y., Shoji, J.Y., Arioka, M., and Kitamoto, K. 2009. Endocytosis is crucial for cell polarity and apical membrane recycling in the filamentous fungus *Aspergillus oryzae*. Eukaryotic Cell *8*, 37-46.

Huang, J., Wu, S., Barrera, J., Matthews, K., and Pan, D. 2005. The Hippo signaling pathway coordinately regulates cell proliferation and apoptosis by inactivating Yorkie, the *Drosophila* Homolog of YAP. Cell *122*, 421-434.

Kaksonen, M., Toret, C.P., and Drubin, D.G. 2005. A modular design for the clathrin- and actin-mediated endocytosis machinery. Cell *123*, 305-320.

Kono, K., Saeki, Y., Yoshida, S., Tanaka, K., and Pellman, D. 2012. Proteasomal degradation resolves competition between cell polarization and cellular wound healing. Cell *150*, 151-164.

Kubler, E., and Riezman, H. 1993. Actin and fimbrin are required for the internalization step of endocytosis in yeast. The EMBO Journal *12*, 2855-2862.

Kukulski, W., and Picco, A. 2016. Clathrin modulates vesicle scission, but not invagination shape, in yeast endocytosis. eLife *5,* e16036.

Kukulski, W., Schorb, M., Kaksonen, M., and Briggs, J.A. 2012. Plasma membrane reshaping during endocytosis is revealed by time-resolved electron tomography. Cell *150*, 508-520.

Kukulski, W., Schorb, M., Welsch, S., Picco, A., Kaksonen, M., and Briggs, J.A. 2011. Correlated fluorescence and 3D electron microscopy with high sensitivity and spatial precision. The Journal of Cell Biology *192*, 111-119.

Lara-Rojas, F., Bartnicki-García, S., and Mouriño-Pérez, R.R. 2016. Localization and role of MYO-1, an endocytic protein in hyphae of *Neurospora crassa*. Fungal Genetics and Biology *88*, 24-34.

López-Franco, R., and Bracker, C.E. 1996. Diversity and dynamics of the Spitzenkörper in growing hyphal tips of higher fungi. Protoplasma *195*, 90-111.

Lu, R., and Drubin, D.G. 2017. Selection and stabilization of endocytic sites by Ede1, a yeast functional homologue of human Eps15. Molecular Biology of the Cell *28*, 567-575.

Lu, R., Drubin, D.G., and Sun, Y. 2016. Clathrin-mediated endocytosis in budding yeast at a glance. The Journal of Cell Science *129*, 1531-1536.

Maldonado-Baez, L., Dores, M.R., Perkins, E.M., Drivas, T.G., Hicke, L., and Wendland, B. 2008. Interaction between Epsin/Yap180 adaptors and the scaffolds Ede1/Pan1 is required for endocytosis. Molecular Biology of the Cell *19*, 2936-2948.

Miesfeld, J.B., and Link, B.A. 2014. Establishment of transgenic lines to monitor and manipulate Yap/Taz-Tead activity in zebrafish reveals both evolutionarily conserved and divergent functions of the Hippo pathway. Mechanisms of Development *133*, 177-188.

Morikawa, Y., Zhang, M., Heallen, T., Leach, J., Tao, G., Xiao, Y., Bai, Y., Li, W., Willerson, J.T., and Martin, J.F. 2015. Actin cytoskeletal remodeling with protrusion formation is essential for heart regeneration in Hippo-deficient mice. Science Signaling *8*, ra41.

Morris, S.A., Schroder, S., Plessmann, U., Weber, K., and Ungewickell, E. 1993. Clathrin assembly protein AP180: primary structure, domain organization and identification of a clathrin binding site. The EMBO Journal *12*, 667-675.

Moseley, J.B., and Goode, B.L. 2006. The yeast actin cytoskeleton: from cellular function to biochemical mechanism. Microbiology and Molecular Biology Reviews *70*, 605-645.

Munn, A.L., Stevenson, B.J., Geli, M.I., and Riezman, H. 1995. end5, end6, and end7: mutations that cause actin delocalization and block the internalization step of endocytosis in *Saccharomyces cerevisiae*. Molecular Biology of the Cell *6*, 1721-1742.

Peñalva, M.A. 2005. Tracing the endocytic pathway of *Aspergillus nidulans* with FM4-64. Fungal Genetics and Biology *42*, 963-975.

Peñalva, M.A. 2010. Endocytosis in filamentous fungi: Cinderella gets her reward. Current Opinion in Microbiology *13*, 684-692.

Petre, B., Saunders, D.G., Sklenar, J., Lorrain, C., Win, J., Duplessis, S., and Kamoun, S. 2015. Candidate effector proteins of the rust pathogen *Melampsora larici-populina* target diverse plant cell compartments. Molecular Plant-Microbe Interactions *28*, 689-700.

Pruyne, D., and Bretscher, A. 2000. Polarization of cell growth in yeast. The Journal of Cell Science *113 (Pt 4)*, 571-585.

Ramos-García, S.L., Roberson, R.W., Freitag, M., Bartnicki-García, S., and Mouriño-Pérez, R.R. 2009. Cytoplasmic bulk flow propels nuclei in mature hyphae of *Neurospora crassa*. Eukaryotic Cell *8*, 1880-1890.

Raths, S., Rohrer, J., Crausaz, F., and Riezman, H. 1993. end3 and end4: two mutants defective in receptor-mediated and fluid-phase endocytosis in *Saccharomyces cerevisiae*. The Journal of Cell Biology *120*, 55-65.

Read, N.D., and Hickey, P.C. 2001. The vesicle trafficking network and tip growth in fungal hyphae. In Cell Biology of Plant and Fungal Tip Growth, A. Geitmann, M. Cresti, and I.B. Heath, eds. (The Netherlands: IOS Press), p. 242.

Read, N.D., and Kalkman, E.R. 2003. Does endocytosis occur in fungal hyphae? Fungal Genetics and Biology *39*, 199-203.

Reider, A., and Wendland, B. 2011. Endocytic adaptors--social networking at the plasma membrane. The Journal of Cell Science *124*, 1613-1622.

Riezman, H. 1985. Endocytosis in yeast: several of the yeast secretory mutants are defective in endocytosis. Cell *40*, 1001-1009.

Riquelme, M., and Bartnicki-García, S. 2008. Advances in understanding hyphal morphogenesis: Ontogeny, phylogeny and cellular localization of chitin synthases. Fungal Biology Reviews *22*, 56-70.

Roberson, R.W. 1992. The Actin Cytoskeleton in Hyphal Cells of *Sclerotium rolfsii*. Mycologia *84*, 41-51.

Roberson, R.W., Abril, M., Blackwell, M., Letcher, P., McLaughlin, D.J., Mouriño-Pérez, R.R., Riquelme, M., and Uchida, M. 2010. Hyphal Structure. In Cellular and Molecular Biology of Filamentous Fungi (American Society of Microbiology).

Sánchez-León, E., Verdin, J., Freitag, M., Roberson, R.W., Bartnicki-García, S., and Riquelme, M. 2011. Traffic of chitin synthase 1 (CHS-1) to the Spitzenkörper and developing septa in hyphae of *Neurospora crassa*: actin dependence and evidence of distinct microvesicle populations. Eukaryotic Cell *10*, 683-695.

Sandrock, T.M., Brower, S.M., Toenjes, K.A., and Adams, A.E. 1999. Suppressor analysis of fimbrin (Sac6p) overexpression in yeast. Genetics *151*, 1287-1297.

Schultzhaus, Z.S., Johnson, T.B., and Shaw, B.D. 2017. Clathrin localization and dynamics in *Aspergillus nidulans*. Molecular Microbiology *103*, 299-318.

Schultzhaus, Z.S., Quintanilla, L., Hilton, A., and Shaw, B.D. 2016. Live cell imaging of actin dynamics in the filamentous fungus *Aspergillus nidulans*. Microscopy and Microanalysis: the Official Journal of Microscopy Society of America, Microbeam Analysis Society, Microscopical Society of Canada *22*, 264-274.

Schultzhaus, Z.S., and Shaw, B.D. 2015. Endocytosis and exocytosis in hyphal growth. Fungal Biology Reviews *29*, 43-53.

Shaw, B.D., Chung, D.W., Wang, C.L., Quintanilla, L.A., and Upadhyay, S. 2011. A role for endocytic recycling in hyphal growth. Fungal Biology *115*, 541-546.

Steinberg, G. 2007. Hyphal growth: a tale of motors, lipids, and the Spitzenkörper. Eukaryotic Cell *6*, 351-360.

Stimpson, H.E., Toret, C.P., Cheng, A.T., Pauly, B.S., and Drubin, D.G. 2009. Early-arriving Syp1p and Ede1p function in endocytic site placement and formation in budding yeast. Molecular Biology of the Cell *20*, 4640-4651.

Sudol, M., Bork, P., Einbond, A., Kastury, K., Druck, T., Negrini, M., Huebner, K., and Lehman, D. 1995. Characterization of the mammalian YAP (Yes-associated protein) gene and its role in defining a novel protein module, the WW domain. The Journal of Biological Chemistry *270*, 14733-14741.

Szubinska, B. 1971. "New membrane" formation in *Amoeba proteus* upon injury of individual cells. Electron microscope observations. The Journal of Cell Biology *49*, 747-772.

Taheri-Talesh, N., Horio, T., Araujo-Bazán, L., Dou, X., Espeso, E.A., Peñalva, M.A., Osmani, S.A., and Oakley, B.R. 2008. The tip growth apparatus of *Aspergillus nidulans*. Molecular Biology of the Cell *19*, 1439-1449.

Takagi, T. 2003. Ultrastructure and behavior of actin cytoskeleton during cell wall formation in the fission yeast *Schizosaccharomyces pombe*. Journal of Electron Microscopy *52*, 161-174.

Togo, T., Alderton, J.M., Bi, G.Q., and Steinhardt, R.A. 1999. The mechanism of facilitated cell membrane resealing. The Journal of Cell Science *112 (Pt 5)*, 719-731.

Torralba, S., and Heath, I.B. 2002. Analysis of three separate probes suggests the absence of endocytosis in *Neurospora crassa* hyphae. Fungal Genetics and Biology *37*, 221-232.

Trinci, A.P. 1969. A kinetic study of the growth of *Aspergillus nidulans* and other fungi. Journal of General Microbiology *57*, 11-24.

Trinci, A.P.J., and Collinge, A.J. 1974. Occlusion of the septal pores of damaged hyphae of *Neurospora crassa* by hexagonal crystals. Protoplasma *80*, 57-67.

Upadhyay, S., and Shaw, B.D. 2008. The role of actin, fimbrin and endocytosis in growth of hyphae in *Aspergillus nidulans*. Molecular Microbiology *68*, 690-705.

Waddle, J.A., Karpova, T.S., Waterston, R.H., and Cooper, J.A. 1996. Movement of cortical actin patches in yeast. The Journal of Cell Biology *132*, 861-870.

Weinberg, J., and Drubin, D.G. 2012. Clathrin-mediated endocytosis in budding yeast. Trends in Cell Biology *22*, 1-13.

Wendland, B., and Emr, S.D. 1998. Pan1p, yeast eps15, functions as a multivalent adaptor that coordinates protein–protein interactions essential for endocytosis. The Journal of Cell Biology *141*, 71-84.

Wendland, J., and Walther, A. 2005. Tip growth and endocytosis in fungi. In Plant Endocytosis, J. Šamaj, F. Baluška, and D. Menzel, eds. (Springer).

Yamashita, R.A., and May, G.S. 1998. Constitutive activation of endocytosis by mutation of myoA, the myosin I gene of Aspergillus nidulans. The Journal of Biological Chemistry *273*, 14644-14648.

Zess, E.K., Jensen, C., Cruz-Mireles, N., De la Concepcion, J.C., Sklenar, J., Stephani, M., Imre, R., Roitinger, E., Hughes, R., Belhaj, K*., et al.* 2019. N-terminal β-strand underpins biochemical specialization of an ATG8 isoform. PLoS Biology *17*, e3000373.

Appendix

Table 5. Recipes of media used in this work.

Culture media	Quantity	Reagent
Vogel's minimum medium (VMM)	20 ml 15 g ddH_2O to 1 L	Vogel's salts 50X Sucrose Add 15 g of agar for solid medium at 1.5%
Vogel's salts 50X	125 g 250 g 100 g 10 g 5 g 5 ml 2.5 ml 755 ml Add ~5 ml chloroform as preservative.	$Na_3C_6H_5O_7 \cdot 2H_2O$ KH_2PO_4 NH_4NO_3 $MgSO_4 \cdot 7H_2O$ $CaCl_2 \cdot 2H_2O$ (dissolved) Trace elements solution Biotin stock solution ddH_2O Store at RT.
Trace elements for Vogel's	5 g 5 g 1 g 0.25 g 0.05 g 0.05 g 0.05 g	$C_6H_8O_7 \cdot H_2O$ $ZnSO_4 \cdot 7H_2O$ $Fe(NH_4)_2(SO_4)_2 \cdot 6H_2O$ $CuSO_4 \cdot 5H_2O$ $MnSO_4 \cdot H_2O$ H_3BO_3 (anhydrous) $Na_2MoO4 \cdot 2H_2O$
Biotin stock solution	5 mg 50 ml	Biotin H_2O or 50% ethanol Store at -20°C
Complete medium (CM)	50 ml 1 ml 10 g 2 g 1 g 1 g 1 ml pH 6.5, ddH_2O to 1 L	20X Nitrate salts Trace elements D-glucose Peptone Yeast extract Casamino acids Vitamin solution

20X Nitrate salts	120 g 10.4 g 10.4 g 30.4 g ddH_2O to 1 L	$NaNO_3$ KCl $MgSO_4 \cdot 7H_2O$ KH_2PO_4 Autoclave and store at 5°C
1000X Trace elements for CM	80 ml 2.2 g 1.1 g 0.5 g 0.5 g 0.17 g 0.16 g 0.15 g 5 g Add the compounds in order. Boil. Cool to 60°C. pH 6.5	ddH_2O $ZnSO_4 \cdot 7H_2O$ H_3BO_3 $MnCl_2 \cdot 4H_2O$ $FeSO_4 \cdot 7H_2O$ $CoCl_2 \cdot 6H_2O$ $CuSO_4 \cdot 5H_2O$ $Na_2MoO4 \cdot 2H_2O$ Na_4EDTA ddH_2O to 100 ml
Vitamin solution	0.01 g 0.01 g 0.01 g 0.01 g 0.01 g 0.01 g 100 ml Store in a dark at 4°C	Biotin Pyridoxin Thiamine Riboflavin PABA (p-aminobenzoic acid) Nicotinic acid ddH_2O

Table 6. Identified proteins in the LC-MS/MS of AP180-GFP.

Identified proteins	ORF name	Molecular weight	AP180/cyto
Uncharacterized protein	NCU08889	204 kDa	179.7
Invertase	NCU04265	75 kDa	6.7
Aldehyde dehydrogenase	NCU03415	54 kDa	6.3
4-amino-5-hydroxymethyl-2-methylpyrimidine phosphate synthase	NCU09345	38 kDa	6.0
12-oxophytodienoate reductase 1	NCU04452	42 kDa	5.3
Acyl-CoA dehydrogenase	NCU02287	61 kDa	4.4
Profilin	NCU06397	14 kDa	4.3
GTP cyclohydrolase II	NCU01449	56 kDa	4.3
UMTA	NCU05841	43 kDa	4.2
Scavenger mRNA decapping enzyme	NCU06998	41 kDa	4.0
Transmembrane 9 superfamily member	NCU07330	72 kDa	4.0

Ubiquitinyl hydrolase 1	NCU03797	134 kDa	4.0
Ribonucleoside-diphosphate reductase large chain	NCU03539	104 kDa	3.7
Signal recognition particle receptor subunit beta	NCU08217	47 kDa	3.7
UPF0135 protein	NCU06108	39 kDa	3.7
Cleavage and polyadenylation specificity factor subunit 5	NCU09014	30 kDa	3.7
Clock-controlled protein 9	NCU09559	96 kDa	3.7
Oxidoreductase	NCU09278	34 kDa	3.3
Vacuolar protein sorting/targeting protein 10	NCU02669	172 kDa	3.3
Autophagy-related protein 27	NCU03543	42 kDa	3.3
Dolichyl-phosphate-mannose--protein mannosyltransferase	NCU09332	88 kDa	3.2
Uracil phosphoribosyltransferase	NCU06261	24 kDa	3.2
Norsolorinic acid reductase	NCU07723	42 kDa	3.0
Amphiphysin-like lipid raft protein	NCU01069	30 kDa	3.0
Protein pbn1	NCU00101	56 kDa	3.0
Importin beta-2 subunit	NCU03690	105 kDa	3.0
Sec23/Sec24 family protein	NCU06868	115 kDa	3.0
D-isomer specific 2-hydroxyacid dehydrogenase	NCU11195	42 kDa	3.0
Thioredoxin-like_fold domain-containing protein	NCU02547	31 kDa	3.0
Uncharacterized protein	NCU05832	44 kDa	3.0
Oxysterol binding protein 1, variant	NCU00579	134 kDa	2.9
Oxidoreductase	NCU09821	33 kDa	2.9
TPR_MLP1_2 domain-containing protein	NCU04059	234 kDa	2.8
CBM21 domain-containing protein	NCU08779	91 kDa	2.8
Uncharacterized protein	NCU04910	41 kDa	2.8
Aldehyde dehydrogenase	NCU07053	54 kDa	2.8
Pre-mRNA splicing factor	NCU07069	37 kDa	2.8
Uncharacterized protein	NCU00295	73 kDa	2.8
SGNH_hydro domain-containing protein	NCU00397	29 kDa	2.8
Diploid state maintenance protein chpA	NCU03087	35 kDa	2.7
Putative mitochondrial 2-oxoglutarate/malate carrier protein	NCU10732	35 kDa	2.7
Uncharacterized protein	NCU10360	59 kDa	2.7
Fumarylacetoacetase	NCU05537	47 kDa	2.7
Uncharacterized protein	NCU11292	22 kDa	2.7
Glutathione transferase omega-1	NCU00549	42 kDa	2.7
Uncharacterized protein	NCU08847	65 kDa	2.7
ATP-dependent RNA helicase dhh1	NCU06149	64 kDa	2.6
Post-transcriptional silencing protein QDE-2, variant	NCU04730	117 kDa	2.6
Uncharacterized protein	NCU04415	62 kDa	2.6
Glycerophosphocholine phosphodiesterase Gde1	NCU01747	138 kDa	2.6
Translation initiation factor eIF-2B subunit delta	NCU01468	50 kDa	2.6

Chitin synthase	NCU04352	208 kDa	2.5
Alpha-aminoadipate reductase	NCU03010	131 kDa	2.5
Two-component system protein A	NCU07221	102 kDa	2.5
Uncharacterized protein	NCU05375	186 kDa	2.5
Microtubule-associated protein RP/EB family member 1	NCU00243	27 kDa	2.5
Bifunctional lycopene cyclase/phytoene synthase	B22I21.230, NCU00585	69 kDa	2.4
SH3 domain-containing protein	NCU07012	130 kDa	2.4
Probable acetate kinase	B12J7.040	51 kDa	2.4
Heat shock protein hsp98	NCU00104	103 kDa	2.4
NmrA family transcriptional regulator	NCU09169	35 kDa	2.4
Aminoacyl-tRNA hydrolase	NCU01501	36 kDa	2.3
Sorbitol utilization protein SOU2	NCU03803	31 kDa	2.3
Chitin synthase	NCU04350	202 kDa	2.3
Oxysterol binding protein	NCU08578	46 kDa	2.3
Ergot alkaloid biosynthetic protein A	NCU07474	37 kDa	2.3
Alpha-1,3-glucan synthase	NCU02478	269 kDa	2.3
Mito ribosomal protein S2	NCU12023	47 kDa	2.3
4-hydroxyphenylpyruvate dioxygenase	B23G1.170	46 kDa	2.3
CipA protein	NCU01138	39 kDa	2.3
Protease inhibitor	NCU06524	28 kDa	2.3
AMPK1_CBM domain-containing protein	NCU03870	87 kDa	2.3
Uncharacterized protein	NCU11291	20 kDa	2.3
Rtg2-like protein		66 kDa	2.3
L-lactate dehydrogenase	NCU00720	35 kDa	2.3
Aspartate aminotransferase	NCU07941	52 kDa	2.3
Transmembrane protein	NCU03263	165 kDa	2.3
DUF636 domain-containing protein	NCU01424	15 kDa	2.3
GTP-binding protein YPT52	NCU06410	25 kDa	2.3
Toxin biosynthesis protein	NCU03925	47 kDa	2.3
Isopentenyl-diphosphate Delta-isomerase	NCU07719	29 kDa	2.3
Alpha-1,3-glucan synthase	NCU08132	265 kDa	2.3
ATP-dependent Zn protease	NCU05160	55 kDa	2.3
Short chain dehydrogenase	NCU02018	32 kDa	2.3
Uncharacterized protein	NCU06265	98 kDa	2.2
Rho-GTPase-activating protein 8	NCU09537	98 kDa	2.2
Hsp90 chaperone protein kinase-targeting subunit	NCU00472	55 kDa	2.2
SNARE protein Ykt6	NCU08973	22 kDa	2.2
Uncharacterized protein	NCU09101	66 kDa	2.2
Uncharacterized protein	NCU06844	26 kDa	2.2
Fumarate reductase Osm1	NCU02580	67 kDa	2.2
Dienelactone hydrolase	NCU09600	32 kDa	2.2
Proteasome activator subunit 4	NCU05620	222 kDa	2.2

Methylenetetrahydrofolate reductase	NCU07690	70 kDa	2.2
WD repeat containing protein 2	NCU03944	64 kDa	2.2
Ribonucleoside-diphosphate reductase small chain	NCU07887	47 kDa	2.2
Uncharacterized protein	NCU00627	68 kDa	2.2
Glucosidase II alpha subunit	NCU04203	112 kDa	2.1
RNA binding protein	NCU02765	13 kDa	2.1
Phosphopantothenate-cysteine ligase	NCU09090	48 kDa	2.1
Mannose-6-phosphate isomerase	103E1.170	50 kDa	2.1
Methionine synthase	NCU10020	43 kDa	2.1
Uncharacterized protein	NCU08095	28 kDa	2.1
Pyruvate decarboxylase	NCU08771	66 kDa	2.1
Long-chain-alcohol oxidase	NCU08977	82 kDa	2.1
Uncharacterized protein	NCU02972	91 kDa	2.1
Uncharacterized protein	NCU09097	105 kDa	2.1
NAD(P)H-hydrate epimerase	NCU08070	26 kDa	2.1
AMP-binding domain-containing protein	NCU01170	62 kDa	2.1
Protein kinase C-like	NCU06544	128 kDa	2.1
Phospholipase A-2-activating protein	NCU06544	88 kDa	2.1
Dolichyl-phosphate-mannose--protein mannosyltransferase	NCU01648	86 kDa	2.1
Uncharacterized protein	NCU05535	34 kDa	2.1
Protein bli-3	NCU07267	23 kDa	2.0
NIMA-interacting protein TinC	NCU03125	90 kDa	2.0
Uncharacterized protein	NCU04522	26 kDa	2.0
Cap binding protein	NCU04187	93 kDa	2.0
UDP-glucose:glycoprotein glucosyltransferase	NCU02349	169 kDa	2.0
Nsp1_C domain-containing protein	NCU02808	67 kDa	2.0
Probable dipeptidyl-aminopeptidase B	NCU02515	104 kDa	2.0
Phosphomevalonate kinase	NCU08671	48 kDa	2.0
Sporulation protein SPS19	NCU07958	33 kDa	2.0
TIM-barrel enzyme family protein	NCU00864	30 kDa	2.0
Porphobilinogen deaminase	B4B2.080, NCU08876, NCU10292	37 kDa	2.0
3-phytase	NCU06460	60 kDa	2.0
Flavoprotein oxygenase	NCU00236	40 kDa	2.0
Uncharacterized protein	NCU02899	57 kDa	2.0
Dipeptidyl-peptidase V	NCU03290	83 kDa	2.0
Signal peptidase subunit 3	NCU06677	25 kDa	2.0
S-methyl-5'-thioadenosine phosphorylase	NCU03963	34 kDa	2.0
Protein transport protein sec13	NCU04063	33 kDa	2.0
Phosphatidylserine decarboxylase proenzyme 2	-	118 kDa	2.0
Non-specific serine/threonine protein kinase	NCU00406	92 kDa	2.0
Eukaryotic translation initiation factor 2A	NCU06099	74 kDa	2.0

Twinfilin-1	NCU16698	37 kDa	2.0
Extracellular serine carboxypeptidase	NCU00831	62 kDa	2.0
Homogentisate 1,2-dioxygenase	NCU05499	52 kDa	2.0
Uncharacterized protein	NCU04917	41 kDa	2.0
Ubiquitin conjugation factor E4	NCU03357	125 kDa	2.0
Methylenetetrahydrofolate dehydrogenase	NCU00963	38 kDa	2.0
Glutamate-5-semialdehyde dehydrogenase	NCU01412	47 kDa	2.0
Phosphoribosylaminoimidazole carboxylase	NCU03194	69 kDa	2.0
NADH-ubiquinone oxidoreductase 21 kDa subunit, mitochondrial	NCU05221	24 kDa	2.0
V-type proton ATPase subunit d	B19C19.060, NCU03395	41 kDa	2.0
Glutathione S-transferase-4	NCU10521	25 kDa	2.0
Succinate-semialdehyde dehydrogenase	NCU00936	58 kDa	2.0
Eukaryotic release factor 1	NCU00410	49 kDa	2.0
Dolichol-phosphate mannosyltransferase subunit 1	NCU07965	27 kDa	2.0
Translation machinery-associated protein 20	NCU08678	24 kDa	2.0
RuvB-like helicase 2	NCU06854	52 kDa	2.0
3-isopropylmalate dehydratase	NCU04385	85 kDa	2.0
Succinyl-CoA:3-ketoacid-coenzyme A transferase	NCU06881	55 kDa	2.0
Phenol 2-monooxygenase	NCU03023	73 kDa	2.0
GTP-binding protein ypt3	NCU01523	24 kDa	2.0
Homoserine kinase	NCU04277	39 kDa	2.0
Glutamate carboxypeptidase	NCU03108	89 kDa	2.0
Dolichyl-diphosphooligosaccharide--protein glycosyltransferase subunit WBP1	NCU00669	52 kDa	2.0
26S proteasome regulatory subunit RPN11	NCU00823	38 kDa	2.0